



5-2004

CFD Modeling of Dynamic Inlet Flow Distortion Generation

Keith Patrick Savage

University of Tennessee - Knoxville

Recommended Citation

Savage, Keith Patrick, "CFD Modeling of Dynamic Inlet Flow Distortion Generation." Master's Thesis, University of Tennessee, 2004.
https://trace.tennessee.edu/utk_gradthes/2179

This Thesis is brought to you for free and open access by the Graduate School at Trace: Tennessee Research and Creative Exchange. It has been accepted for inclusion in Masters Theses by an authorized administrator of Trace: Tennessee Research and Creative Exchange. For more information, please contact trace@utk.edu.

To the Graduate Council:

I am submitting herewith a thesis written by Keith Patrick Savage entitled "CFD Modeling of Dynamic Inlet Flow Distortion Generation." I have examined the final electronic copy of this thesis for form and content and recommend that it be accepted in partial fulfillment of the requirements for the degree of Master of Science, with a major in Aerospace Engineering.

Dr. Gary Flandro, Major Professor

We have read this thesis and recommend its acceptance:

Dr. Frank Collins, Dr. Joseph Majdalani

Accepted for the Council:

Dixie L. Thompson

Vice Provost and Dean of the Graduate School

(Original signatures are on file with official student records.)

To the Graduate Council:

I am submitting herewith a thesis written by Keith Patrick Savage entitled “CFD Modeling of Dynamic Inlet Flow Distortion Generation.” I have examined the final electronic copy of this thesis for form and content and recommend that it be accepted in partial fulfillment of the requirements for the degree of Master of Science, with a major in Aerospace Engineering.

Dr. Gary Flandro
Major Professor

We have read this dissertation and
recommend its acceptance:

Dr. Frank Collins

Dr. Joseph Majdalani

Acceptance for the Council:

Anne Mayhew
Vice Provost and Dean of Graduate
Studies

(Original signatures are on file with official student records.)

CFD Modeling of Dynamic Inlet Flow Distortion Generation

A Thesis Presented
for the Master of Science Degree
The University of Tennessee, Knoxville

Keith Patrick Savage
May 2004

Acknowledgments

I would like to thank my advisory committee for their support and advice in the course of this study, particularly for Dr. Gary Flandro for putting me on this path and keeping me on track. His curiosity and enthusiasm kept me from getting discouraged during the more challenging periods.

Dr. Charles Merkle improved my understanding of CFD and gave me a great deal of ideas, suggestions and advice on the development of the grid itself and the interpretation of the results.

The nameless, faceless “nparc-support@info.arnold.af.mil” helped me past an insurmountable problem of my own doing with patience and understanding.

The CFD software being used was developed to run on *nix systems, but my prior experience with Linux was minimal. Dr. Ken Kimble’s knowledge and enthusiasm made a believer of me.

Many others contributed to this, however indirectly. Dr. Stephen Liu offered me a great deal of good advice during my four years of undergraduate work, not least of which was the idea of post-graduate education, and Dr. Chester Van Tyne pushed me over the edge with my Senior Thesis project. My parents, family and friends have all been very supportive, encouraging me and keeping me going. I couldn’t have done this without them.

Abstract

Integrating a jet engine into an airframe involves many design and testing steps. The development of high performance fighter aircraft has added new requirements to this process. Ground test facilities are used to simulate the effect of inlet shape on the performance of an engine for cruise flight or other fixed conditions. While a static simulation of the inlet shape is adequate for most circumstances, military fighter craft are highly maneuverable, altering the inlet airflow intensely and briefly. These transient distortions can have a significant impact on performance as well as having the potential of causing structural problems. In addition to airflow changes caused by flight maneuvers, the release of weapons stores into the airstream can introduce transient turbulence and add exhaust gas contaminants. Currently, none of these transient effects are evaluated in wind tunnel ground tests.

One solution that has been proposed to address this issue is an array of individually controlled wedges placed in the wind tunnel ahead of the test engine. The wedges could be opened and closed, not only to simulate the given inlet shape, but also transient distortions. Coupled with a system to introduce contaminants into the flow, all manner of transient and static inlet flow distortions could be simulated in a controlled environment.

Some investigations have already developed mathematical models of variable angle wedges in a free stream and validated those models with experimental data. If these real world experimental results can be duplicated in a CFD model then ultimately the entire wedge array can be developed virtually to arrive at an optimum design with a relatively small investment. To that end, this study focused on developing a two dimensional CFD model to provide solution data to compare with experimental results in order to determine the feasibility of a more elaborate CFD model as a development tool for the wedge array distortion generator.

Table of Contents

1	Introduction	1
2	Literature Review and Previous Work	2
2.1	Transient Distortion Generator	2
2.2	Wake Characteristics	3
3	CFD Model Setup	4
3.1	Wedge Geometry	4
3.2	Grid Design	6
3.3	Turbulence Model	10
3.4	Running <i>Wind</i>	10
4	Test Results	11
4.1	Stability Analysis	11
4.2	Development of the Solution	13
4.3	Comparison with Prior Test Data	13
5	Conclusions and Recommendations	18
5.1	Conclusions	18
5.2	Recommendations	18
	References	24
	Appendices	26
A	Grid Development	27
A.1	Wedge Geometry	27
A.2	Wind Tunnel Test Section Geometry	28
A.3	Boundary Layer Thickness	28

A.4	Geometric Progression	29
A.5	<i>Plot-3D</i> Grid File Format	30
A.6	Other Concerns	31
B	Sample Code and Parameters	32
B.1	Generating the Grid (MatLab m-file)	32
B.2	Sample Run Parm's (<i>wind</i> dat file)	39
B.3	Running <i>Wind</i> Multiple Times (REXX script)	40
B.4	Pressure and Velocity Data Extraction (REXX script)	41
B.5	Clean-up <i>Cfpost</i> Output (REXX script)	42
B.6	Displaying "Surfaces" (MatLab m-file)	43
C	Tools	51
C.1	<i>Cfcvnt</i> (version 1.45)	51
C.2	<i>Gman</i> (version 6.153)	51
C.3	<i>Wind</i> (version 5.193)	51
C.4	<i>Resplt</i> (version unknown)	52
C.5	<i>Cfpost</i> (version 3.163)	52
D	Results	53
D.1	Solution and Convergence, 30° Wedge	54
D.2	Solution and Convergence, 60° Wedge	57
D.3	Solution and Convergence, 90° Wedge	60
D.4	Solution and Convergence, 120° Wedge	63
D.5	Solution and Convergence, 150° Wedge	66
Vita	69

List of Tables

4.1 A comparison of results from each test case 14

5.1 Summary of recommendations for future work 23

List of Figures

2.1	Proposed transient distortion generator	2
3.1	Photo of actual “wedge” used in the Eddy study	5
3.2	Comparison of the experimental wedge and the computer model	5
3.3	The first multi-zone grid with a very simple 90° wedge geometry	8
3.4	A grid with wedge chimera overlay	9
3.5	The final grid format	9
4.1	Sample output from <i>wind</i>	11
4.2	<i>Navier-Stokes</i> L_2 convergence for 90° wedge run	12
4.3	L_2 convergence for the SST calculations	12
4.4	Total pressure calculated at different iterations	15
4.5	Original pressure coefficient contour data from the Eddy study	16
4.6	A comparison of measured and calculated pressure coefficient values	17
5.1	Close-up of the lower wedge tip	19
5.2	A contour plot of the average velocity	20
5.3	Sections needed to evaluate flow coupling for wedge pairs	22
A.1	The modified door hinge used by Eddy	27
A.2	The Lexan test section used in the Eddy study	28
D.1.1	Convergence data for <i>Navier-Stokes</i> calculations for the 30° wedge run	54
D.1.2	Convergence data for <i>Shear Stress Transport</i> calculations, 30° wedge run	54
D.1.3	Total pressure values for 30° wedge after 10,000 iterations	55
D.1.4	Average velocity values for 30° wedge after 10,000 iterations	55
D.1.5	Comparison of pressure coefficient data for 30° wedge	56
D.2.1	Convergence data for <i>Navier-Stokes</i> calculations for the 60° wedge run	57
D.2.2	Convergence data for <i>Shear Stress Transport</i> calculations, 60° wedge run	57
D.2.3	Total pressure values for 60° wedge after 10,000 iterations	58
D.2.4	Average velocity values for 60° wedge after 10,000 iterations	58
D.2.5	Comparison of pressure coefficient data for 60° wedge	59

D.3.1	Convergence data for <i>Navier-Stokes</i> calculations for the 90° wedge run	60
D.3.2	Convergence data for <i>Shear Stress Transport</i> calculations, 90° wedge run	60
D.3.3	Total pressure values for 90° wedge after 10,000 iterations	61
D.3.4	Average velocity values for 90° wedge after 10,000 iterations	61
D.3.5	Comparison of pressure coefficient data for 90° wedge	62
D.4.1	Convergence data for <i>Navier-Stokes</i> calculations for the 120° wedge run	63
D.4.2	Convergence data for <i>Shear Stress Transport</i> calculations, 120° wedge run	63
D.4.3	Total pressure values for 120° wedge after 10,000 iterations	64
D.4.4	Average velocity values for 120° wedge after 10,000 iterations	64
D.4.5	Comparison of pressure coefficient data for 120° wedge	65
D.5.1	Convergence data for <i>Navier-Stokes</i> calculations for the 150° wedge run	66
D.5.2	Convergence data for <i>Shear Stress Transport</i> calculations, 150° wedge run	66
D.5.3	Total pressure values for 150° wedge after 10,000 iterations	67
D.5.4	Average velocity values for 150° wedge after 10,000 iterations	67
D.5.5	Comparison of pressure coefficient data for 150° wedge	68

1 Introduction

Jet engines go through many development and testing steps before actually being installed in an aircraft. Once a bare engine is optimized for ideal operating conditions, it is submitted to ground tests to evaluate its performance after it is placed in an airframe. Various methodologies are used in wind tunnel tests to cause distorted flow upstream of the compressor face to simulate a particular inlet shape. These simulated inlet flow distortions, at present, only simulate a fixed inlet form over a range of flow velocities. This is more than adequate for conventional aircraft engines, but high performance systems like those in military fighter craft have a much broader operating envelope that is not sufficiently tested with current approaches. Fighter craft are necessarily more powerful and maneuverable and the latest generation supplements control surfaces with vectored thrust to enhance that maneuverability even further. These dramatic changes in orientation distort the inlet flow drastically and briefly, disrupting engine performance and possibly even damaging components. An additional concern is the transient disruptions that occur when weapons are released and they and their exhaust gases pass through the inlet stream. Currently, there is no single, comprehensive and robust methodology to simulate these situations during wind tunnel testing.

One possible solution to this is the use of an array of individually controlled wedges placed in the wind tunnel ahead of the engine being tested. This array could replace existing methods for static testing and allow for more complicated testing as well. The wedges could be closed completely, causing no significant distortions, then selectively opened and closed to simulate a transient distortion. Simulated contaminants could also be introduced to the stream as well, with the wedges providing mixing like the v-gutters in an afterburner. Taken all together, this wedge array system could replace existing methodologies while providing an immensely broader range of simulation possibilities.

Many studies of air flow around bluff bodies have provided a starting point for mathematical models of wedges, and wind tunnel experiments have corroborated those results. An obvious next step is to determine if a CFD model can be used to develop the array.

2 Literature Review and Previous Work

Current inlet flow simulations are static, and inadequate for highly maneuverable fighter craft. Development of a method for generating dynamic distortions in the inlet flow during ground tests would greatly enhance the usefulness of wind tunnel testing.

2.1 Transient Distortion Generator

One possible solution to the problem of generating a transient flow distortion in a wind tunnel is through the use of an array of wedges (Figure 2.1) which could be controlled individually. This would allow a large variety of configurations and could generate both transient and static patterns to simulate virtually any flow distortion imaginable. Supplemented with a system to feed “contaminated” air from the wedges could not only simulate the turbulence of stores release, but also the effects of weapon exhaust gases introduced into the inlet stream.

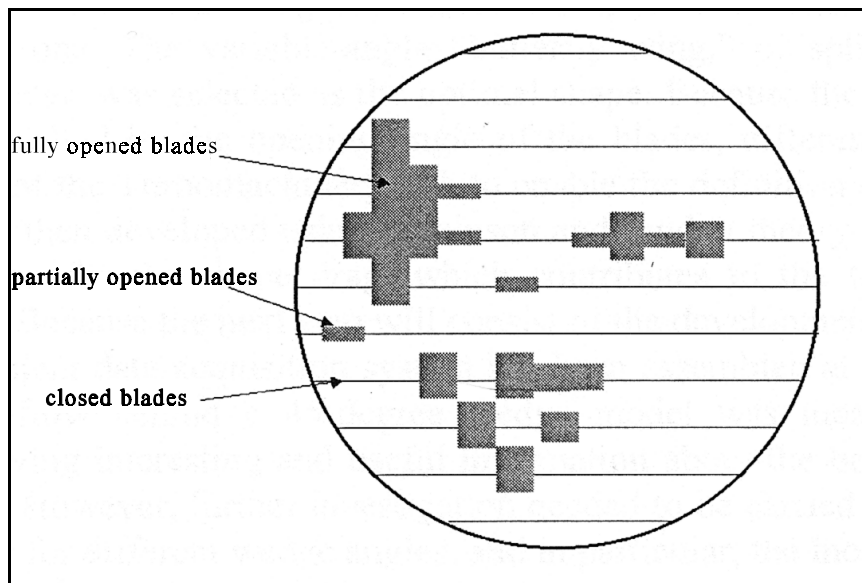


Figure 2.1 Proposed transient distortion generator. The design uses an array of individually operated wedges to vary flow through a wind tunnel [1].

2.2 Wake Characteristics

Flow past wedges and other bluff bodies has been well characterized [2-4], as has flow around aircraft inlets [5, 6]; the ultimate goal is to use the former to simulate the latter. To verify the basic concept, a study at Virginia Polytechnic Institute developed mathematical models to represent the wake characteristics of airflow around a wedge. Then those models were verified with wind tunnel tests, first of a splitter plate, then a series of individual solid wedges [1]. This was followed by a second study focusing on more complex arrangements and more measurements being taken closer to the wedge [7]. Using a modified door hinge for the wedges, simple arrays were easily set up and modified, ultimately showing that wedges could be used to generate consistent and predictable results.

3 CFD Model Setup

A computer-based simulation of the wedge array, based on previous work, that could be modified and reconfigured “virtually” would greatly assist in developing an optimal design. To ensure that a CFD model can provide the required results, it should be shown that a CFD model can re-create the experimental results achieved at Virginia Polytechnic. *Wind* was selected as the CFD modeling tool, owing to its flexibility, applicability and easy access to developers and support. *Wind* is built from the code of three older CFD systems; NASTD from McDonnell Douglas, NPARC from the NPARC Alliance, and NXAIR from AEDC. Taken together, these parts combine to form a very powerful and comprehensive tool.

Before running *wind*, a grid must be supplied that includes the relevant wedge geometry and boundary conditions. *Wind* allows for a number of different turbulence models, so an optimal one must be selected. Finally, execution parameters must be set to mimic the experimental conditions being simulated.

3.1 Wedge Geometry

The wedge used by Eddy started out as a stock steel door hinge [7]. The sixteenth inch thick hinge was trimmed down to one and an eight inches long and two inches wide when fully open (see Figure 3.1). The hinge was mounted in the twelve by twelve inch wind tunnel on a one eighth inch diameter rod (replacing the hinge pin) and then set to a specific angle and locked into place with set screws on the downwind side of the hinge.

For this study, the wedge model geometry was simplified. The hinge itself was treated as a smooth, continuous surface on the front and back, and the back of the hinge merges directly into the “flap” at right angles (see Figure 3.2).

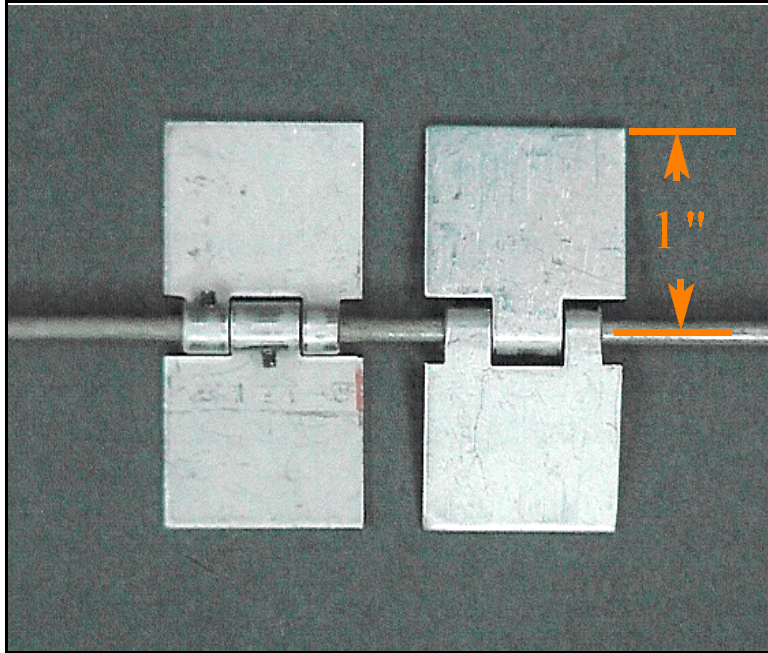


Figure 3.1 Photo of the actual “wedge” used in the Eddy study. Note that multiple wedges can be mounted on the support rod which spans the width of the wind tunnel [7].

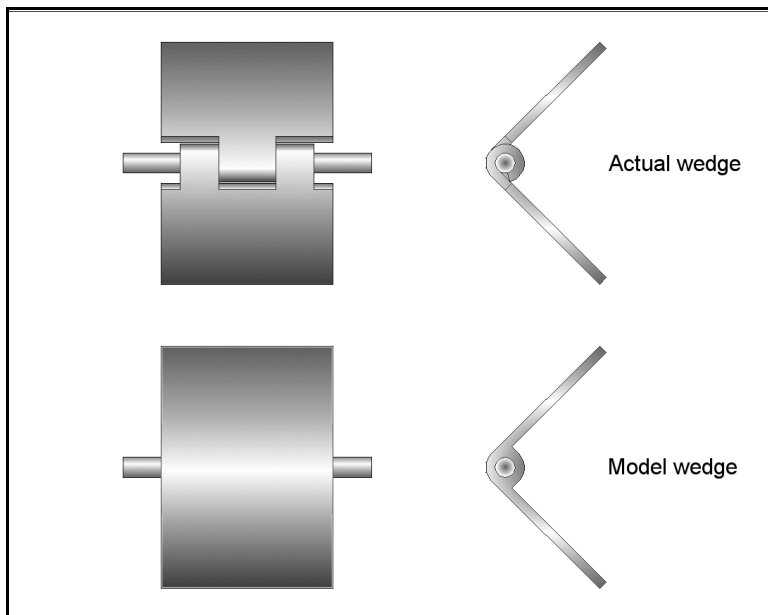


Figure 3.2 Comparison of the experimental wedge and the computer model. The complexity of the hinge area was greatly simplified.

Because the hinge axis is offset by an eighth of an inch from the upwind surface, the model must also allow for the hinge area to “shift” from back to front as the wedge angle decreases. In other words, when the wedge is fully open, the hinge is only exposed on the back. But as the wedge closes, an increasing part of the hinge is exposed on the upwind side, while the exposed hinge decreases on the downwind side, e.g. the quarter cylinder area of the hinge exposed on the upwind edge of the 90° wedge in Figure 3.2.

3.2 Grid Design

At the heart of a CFD model is the grid; an array of points that represent position, pressure, velocity, and other related data. While tools are available to generate grids, it seemed more appropriate to build one from scratch for such a relatively simple geometry. This would provide a good fit and improve the understanding of the results. The *wind* reference included an example of Fortran code that would build a three zone Cartesian structured grid representing a simple 2-D expanding duct [8]. While Fortran is powerful, it is also a compiled language which can make development of new code time consuming and visualization and debugging difficult. MatLab is a software product well suited for computation and visualization with an interpreted programming language designed to easily handle matrices. This made it an obvious choice for prototyping a grid, while still leaving the option of later translation to Fortran as needed.

Once a grid is created and saved into an appropriate format, it must be converted to the “common grid format” used by *wind* with the *cfcvnt* tool provided. Then *gman* is used to define the boundaries of each zone and preparing the grid for input into *wind*. Boundaries that are shared between zones are coupled, while each of the outer boundaries are defined as freestream, inlet, or outflow and the boundaries of the wedge itself are defined as viscous walls.

The grid concept went through many changes in the course of development. The first, simplest grid was just drawn around an angled line, with the grid drawn either

parallel or perpendicular to the wedge surface. This was easy to set up, but the wedge geometry was unrealistically simple and the grid size would change dramatically over the range of wedge angles to be studied. This approach was quickly abandoned, but the geometric series approach used to alter the grid size near the surface of the wedge survived through the final grid code (see section A.4 and Figure 3.3).

The next grid attempted to describe a more realistic wedge and attempted to make use of the ‘cut’ option in *gman*; the intent was to stretch a grid around a wedge shaped hole, then use *gman* to define the hole as a viscous boundary. Unfortunately, the ‘cutting’ tool in *gman* is intended to remove a portion of an existing grid to make room for an overlain chimera (a c-type grid wrapped around a complex geometry) and was unsuitable for the intended purpose. The third iteration used the existing grid and a simple chimera (see Figure 3.4). This actually generated a seemingly usable grid, but a test run with *wind* showed that there were still problems. Initially, the grid seemed to be at fault since *wind* failed when it calculated a negative pressure at the lower wedge tip. Eventually it was determined that the problem was in the actual format of the grid file, but by the time this became clear, a new grid code had already been written.

The final approach used ten zones in all, with individual zone edges defining the viscous boundary surfaces of the wedge and additional zones filling the gaps. This also made it simple to define additional downwind zones that were coarser where less detail was needed (see Figure 3.5).

In addition to describing the wedge, the grid also needed to provide data for comparison to the Eddy study. The seven slots used for testing in that study, the first one inch behind the wedge and the remaining every two inches thereafter, dictated the length of the grid, while the height captures the five inch test area plus a one inch buffer on either side.

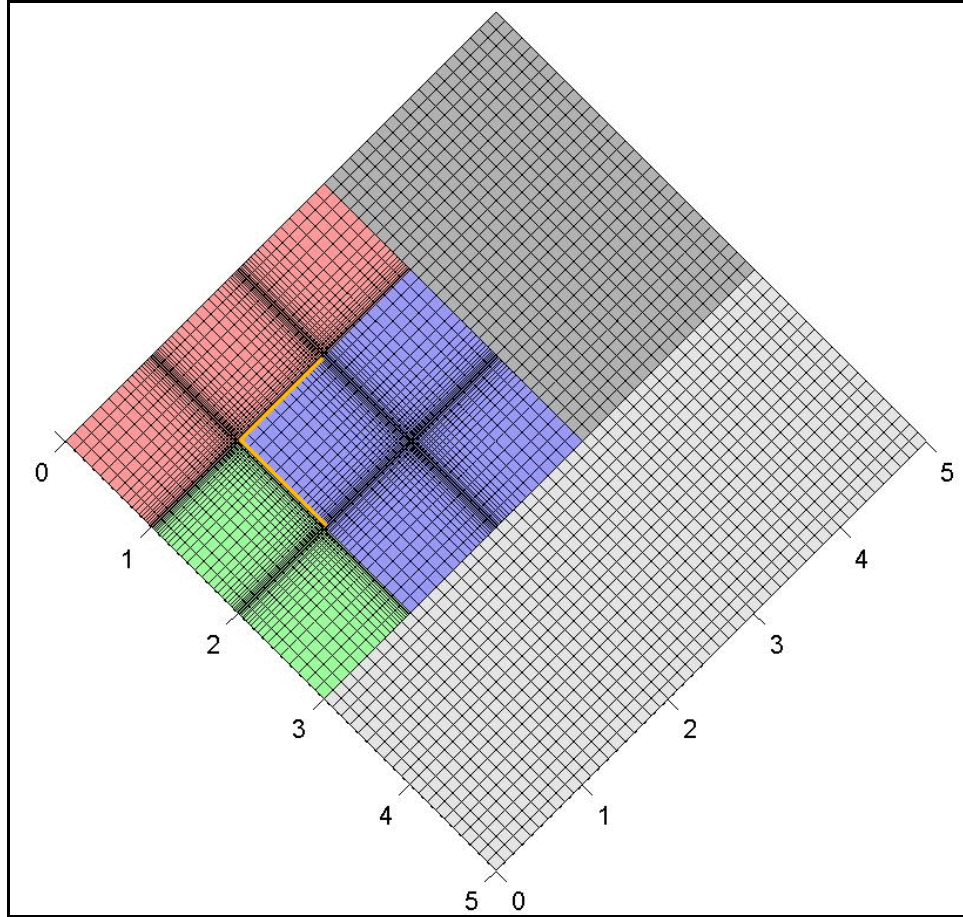


Figure 3.3 The first multi-zone grid with a very simple 90° wedge geometry. The geometric progression routine that shrinks the grid near the surface remained in use for all the following codes.

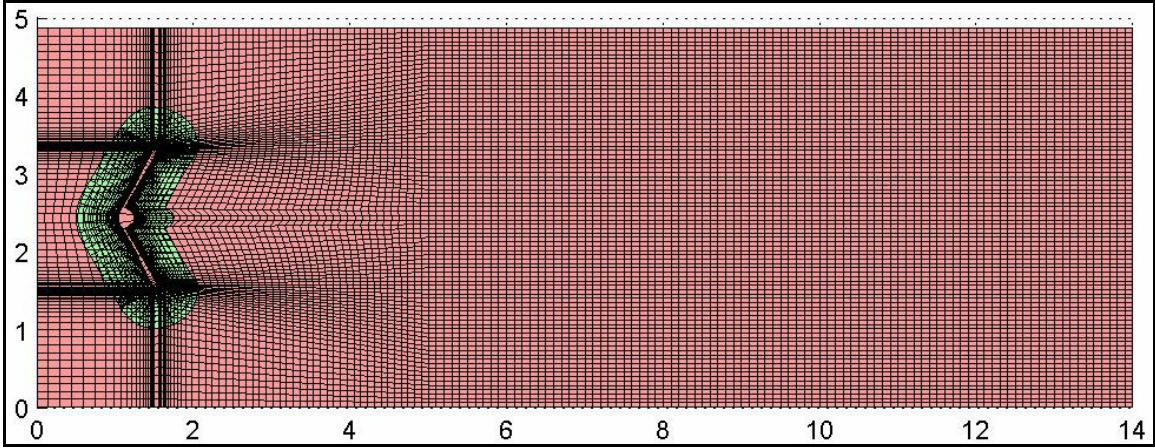


Figure 3.4 A grid with wedge chimera overlay. Errors in the test run led to this being abandoned, but the problem was later determined to be with the file writing routine rather than the grid.

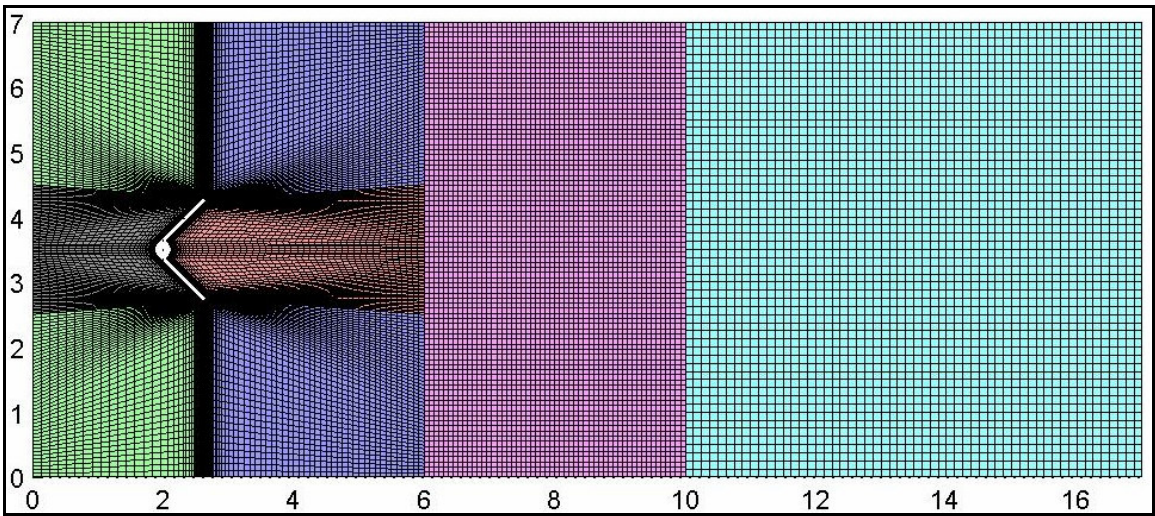


Figure 3.5 The final grid format. Ten zones were created, four with faces defining the wedge surface, four to fill the resulting corners, and two downwind grids of progressively coarser size to reduce the number of points to calculate. (Note: the two zones defining the wedge tip boundaries are obscured by grid lines at this resolution. One extends from the upper wedge tip to the top boundary, the other from the lower tip to the bottom boundary.)

3.3 Turbulence Model

Wind can be run with a number of different turbulence models, from simple (inviscid or laminar) or algebraic (Cebici-Smith or Baldwin-Lomax) to energy equation models like Spalart-Allmaras or Chien. Because of the geometry of the wedge and the unsteady nature of the simulation (due to shedding), the two equation Shear Stress Transport (SST) model was selected. This option incorporates the k - ω model (where k is the specific kinetic energy of the turbulence flux and ω is the dissipation per unit of turbulent kinetic energy) described by Wilcox [9].

3.4 Running Wind

Wind is invoked from the command line, either interactively or in a batch mode. The interactive mode can be invoked either as a prompted command line or as a crude graphical interface. Either of the interactive modes serve well enough for development, but once the appropriate options are identified, the batch mode can be used with scripts to simplify execution. For this study a script was used not only to simplify execution, but to take “snapshots” of the solution during execution (see section B.3). The script invoked *wind* multiple times for short runs, copying the solution file between runs. This made it possible to view the solution as it developed, as well as the final results, which greatly simplified the attendant analysis.

In addition to a properly formatted grid file, *wind* must be provided a set of execution parameters in a simple text file. This “dat” file is used to specify values for free stream conditions, turbulence models, and many other options designed to cover a very broad range of simulated conditions (see section B.2 and the *Wind Users Guide* chapter 10). For this study, free stream values were set to ambient temperature and pressure air, flowing at Mach 0.125 (~42 m/s to match the wind tunnel used in the Virginia Tech studies [1,7]). Downstream values were set to match the free stream and the turbulence model set to SST.

4 Test Results

Test runs of 10,000 iterations each were carried out at five different wedge angles, from 30° to 150° in 30° steps, corresponding to the data provided in Eddy’s work.

4.1 Stability Analysis

The tool *resplt* is used to extract convergence data from the output generated by each *wind* run. The convergence data is then saved in a “genplot” format which can be read and displayed by *cfpost*. The output from *wind* includes “big” and L_2 norms of the residual for each type of calculation; *Navier-Stokes* for all flows, and the specified turbulence model (Shear Stress Transport in this study). A sample of this output can be seen in Figure 4.1.

The plots in Figures 4.2 and 4.3 show typical results. After a period of around 4000 iterations both the *Navier-Stokes* and *SST* calculations settle down. The *SST* convergence for the different zones then starts drifting back up for some zones for the next 2500 iterations or so as the vortices are shed and travel downwind. Zones 3 and 4

```

Beginning flow solution

Zone work memory requirements:
      Single precision      Double precision      Integer
zone  --global--  ---local--  --global--  ---local--  --global--  ---local--
1      71318      419870      8568      28560      4178      5712
ZONE 1 (42x68)
CYCLE  ITER  ZONE  IERR  JERR  KERR  NERR  BIG      L2      CFL|DT
*RES*  421  2101  1    37    2    1    5  -4.211E-04  3.592E-05  1.300E+00
*SST*  421  2101  1    41   14    1    1   8.362E-07  4.996E-08  sst
*RES*  421  2102  1    40    2    1    5  -2.028E-04  3.319E-05  1.300E+00
*SST*  421  2102  1    41   14    1    1   8.374E-07  5.040E-08  sst
*RES*  421  2103  1    41    9    1    5  -1.524E-04  3.292E-05  1.300E+00
*SST*  421  2103  1    41   15    1    1   8.383E-07  5.068E-08  sst
*RES*  421  2104  1    41   10    1    5  -1.585E-04  3.339E-05  1.300E+00
*SST*  421  2104  1    41   15    1    1   8.409E-07  5.081E-08  sst
*RES*  421  2105  1    41   10    1    5  -1.637E-04  3.413E-05  1.300E+00
*SST*  421  2105  1    41   15    1    1   8.417E-07  5.079E-08  sst
ZONE 1:Min/Max CFL = 1.300E+00 1.300E+00 Min/Max DT = 6.643E-08 5.628E-06 sec

```

Figure 4.1 Sample output from *wind*. The residual data displayed here is extracted by the tool *resplt*. The output also includes ranges of CFL and *dt* used along with other data for each zone processed.

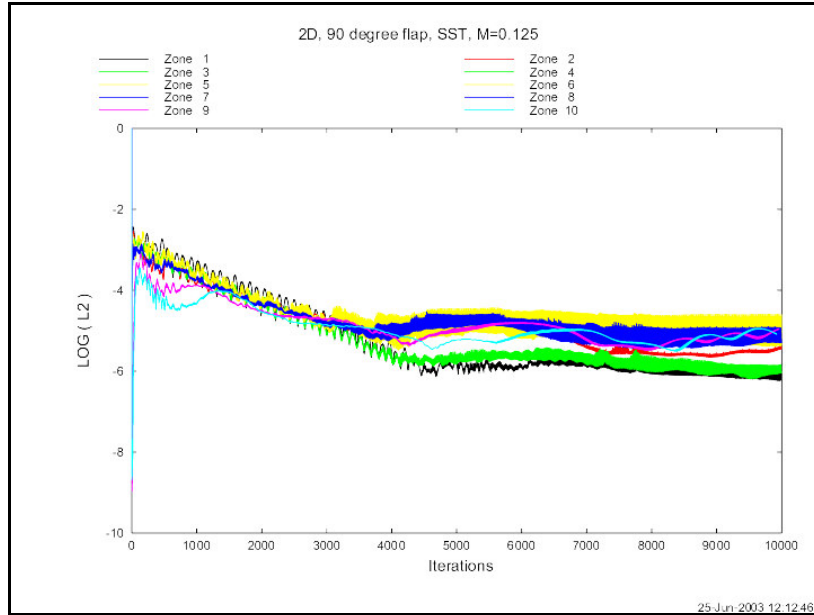


Figure 4.2 Navier-Stokes L_2 convergence for the 90° wedge run. The calculations settle down after 4000 iterations, but converge only to an order ranging from -4 to -6 depending on the zone.

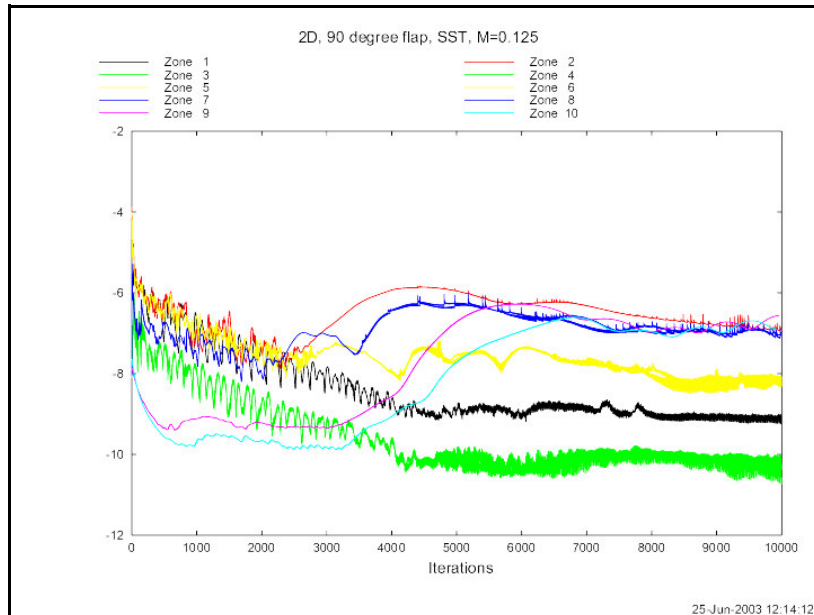


Figure 4.3 L_2 convergence for the SST calculations. These values reflect the complexity of the calculations. Zones 1, 3 and 4 (upstream of the wedge) are clearly unaffected by downstream turbulence.

have the smallest L_2 norm value since they are upwind of the wedge and only “see” a small amount of turbulence at the corner of the wedge tip. Zone 1 has the next smallest L_2 since only the upwind surface of the wedge will generate turbulence. This will probably change at higher velocities as the flow will shift from more laminar to more turbulent. Zones 5 and 6 also “see” only small part of the wedge tip, but it is also the grid that captures the flow separation. Zones 2, 7 and 8 are where the vortices develop, complicating the calculation, and zones 9 and 10 lag behind until the initial vortices travel into them.

4.2 Development of the Solution

Blunt bodies in a freestream typically develop an oscillating flow behavior known as vortex shedding. It was expected that the solution calculated by *wind* would exhibit this phenomena once the computations stabilized. This left the question of how many calculations it would take to reach that point.

From the “snapshots” and the convergence data (as seen in Table 4.1 and Figure 4.4) the answer is clear. It took roughly a thousand iterations for vortices to clearly form, depending on wedge angle, then another three thousand for the remaining flow to stabilize, then another twenty-five hundred for the shedding behavior to take shape. Once the shedding began in earnest and the vortices moved into the trailing regions, the convergence settled down and was consistent for the remaining iterations that were run.

4.3 Comparison with Prior Test Data

Since the original data from Eddy’s work was unavailable, it was necessary to extract values from the figures provided in his appendix (Figure 4.5 is typical). The contour plots of pressure coefficient were scanned, enlarged and printed so values could be determined by eye.

Table 4.1 A comparison of results from each test case. The iteration counts are extracted from the convergence data and pressure images. Test cases were all run on a 1.3 GHz AMD Duron processor with 384 MB RAM, running Linux 2.4.

Wedge angle	Run time [minutes]	Stable vortices form [iterations]	Shedding begins [iterations]
30°	284	3300	4500
60°	273	3400	5000
90°	253	3600	5500
120°	264	3800	6000
150°	267	4000	6500

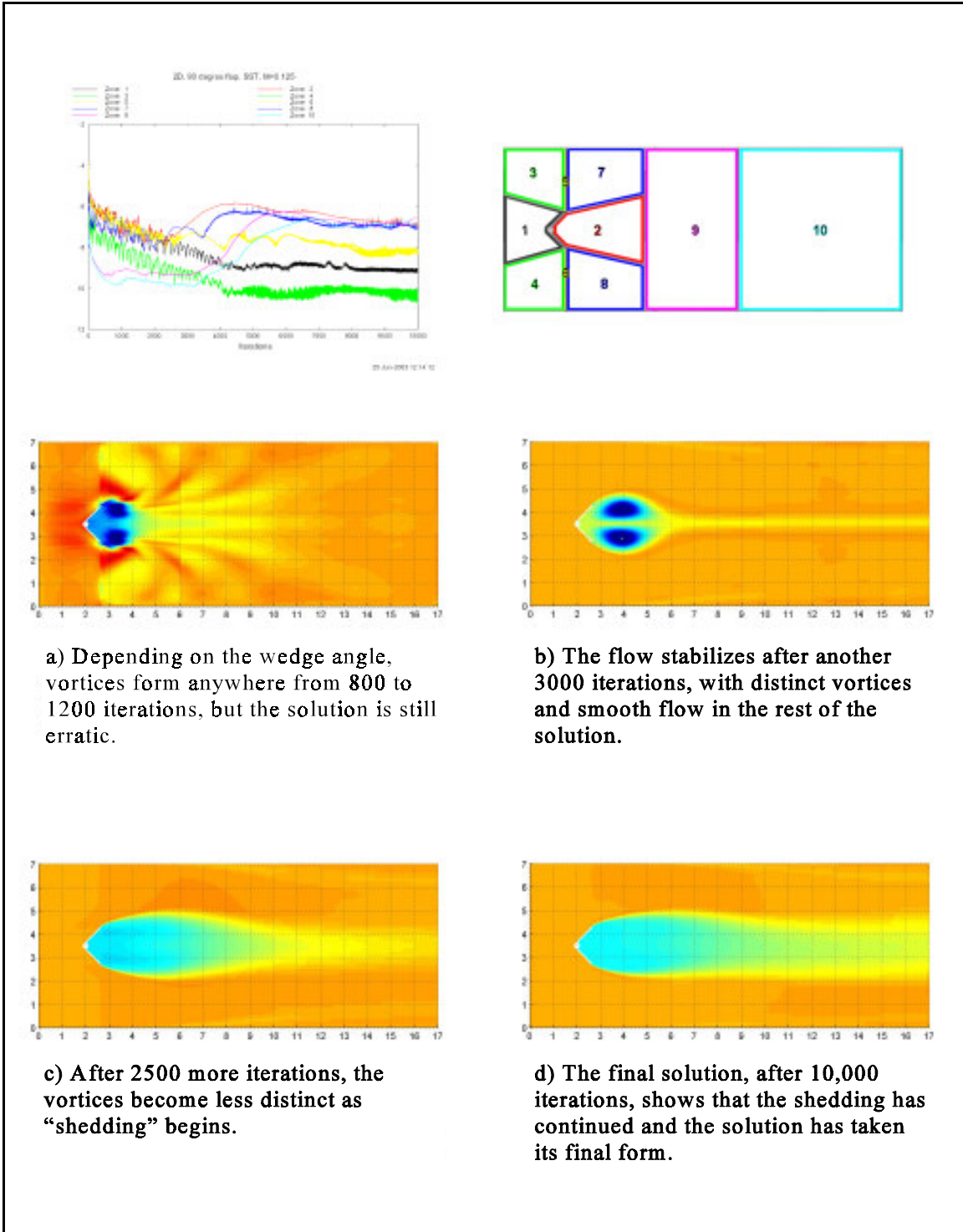


Figure 4.4 Total pressures calculated at different iterations. The convergence data can be seen to “follow” the formation and shedding of the vortices.

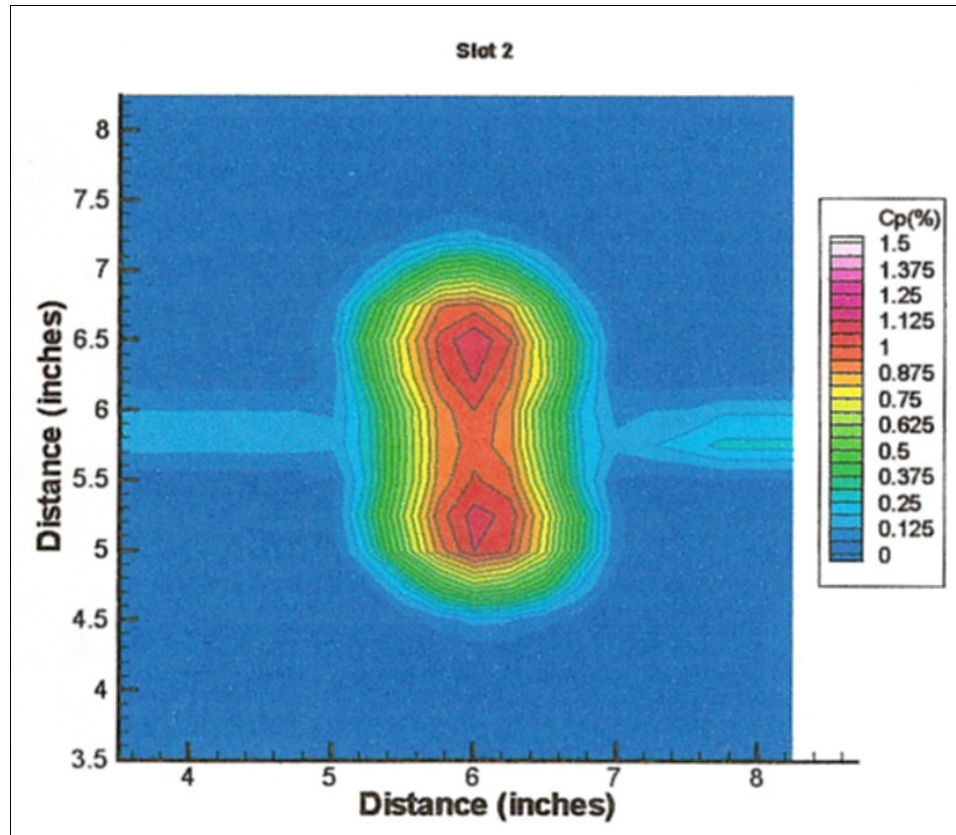


Figure 4.5 Original pressure coefficient contour data from the Eddy study [7]. This example is from the 90° wedge test, slot 2 (3" behind the wedge).

For comparison, pressure values at the appropriate distances were extracted from the pressure data of the CFD model for the last 30 runs and averaged. This encompassed a total of three thousand iterations taken from well after the solution had fully developed. Since the maximum pressure used to determine the pressure coefficient in Eddy's work was unknown, the experimental results were normalized with the largest value found in the Eddy data.

The results (as seen in Figure 4.6) are compelling. The shape, characteristic of shedding flow, is clear in both the measured and calculated values. Downstream measurements showed the same form, but the computed values were greater in magnitude owing to the faster dissipation in three dimensions.

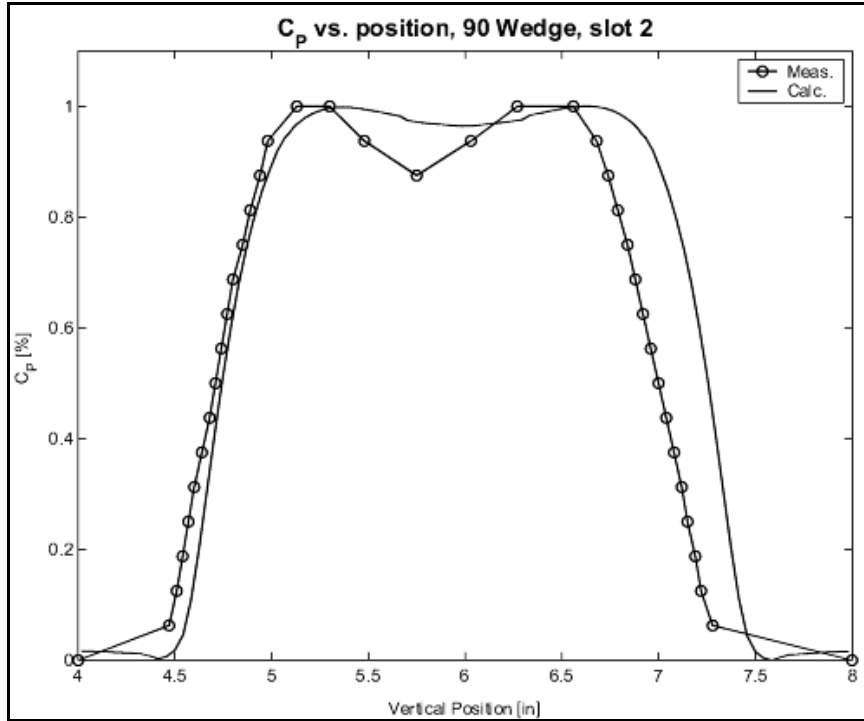


Figure 4.6 A comparison of measured and calculated pressure coefficient values. The calculated values were averaged spanning 3000 iterations (30 samples), then normalized to the largest measured value (since the measured maximum pressure was unavailable). The position is the y-axis distance from the bottom of the wind tunnel at test slot 2, three inches downstream of the wedge.

5 Conclusions and Recommendations

While this study has focused on 2-D, single wedge simulations, it has demonstrated that the modeling concept is sound and also revealed some possible limitations of the wedge-as-distortion-generator concept.

5.1 Conclusions

Placing a wedge in a free stream is essentially a bluff-body problem and the CFD solution showed the classic time dependent vortex shedding behavior expected [2, 10]. Comparing the calculated values to those measured by Eddy showed a good match, right down to the classic “dimple” in the center.

Because this study only modeled a single wedge in two dimensions, it did not answer all questions, but it has shown that the model is sound and will prove useful in the development of a comprehensive and robust simulation of a dynamic distortion generator.

5.2 Recommendations

It may be possible to improve the grid (and achieve better convergence values) by altering the grid geometry at the wedge tips to curve towards the corners so that the grid “lines” at the tips are perpendicular, rather than angled (see Figure 5.1). This “body fitted” approach would help concentrate grid points where the flow separation occurs, at the leading wedge tip, rather than being spread more uniformly across the upwind surface. Alternately, the use of chimeras could be re-evaluated, improving the grid at the wedge tips as well as collapsing zones one through eight into a single background zone and the chimera. Finally, this study relied on a structured Cartesian grid, but an unstructured “mesh” grid could well prove to be as effective and more scalable when the work extends to three dimensions.

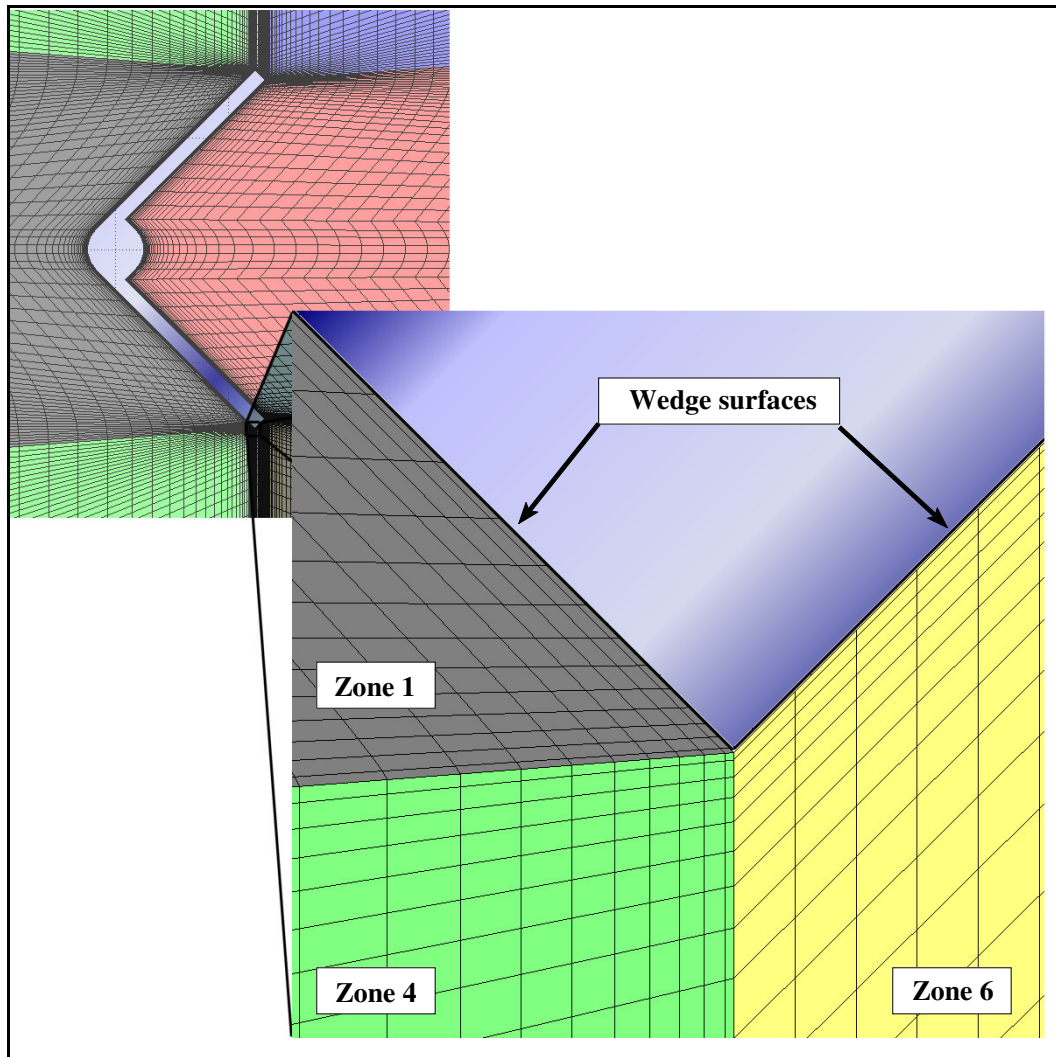


Figure 5.1 Close-up of the lower wedge tip. This reveals the two sets of grid lines which run either parallel or intersect at an angle to the wedge surface.

One issue that appeared in the final analysis and should be addressed before the next phase of investigation is the grid size. Examining the average velocity profiles, it is clear that the velocity entering the grid is being “forced” to a lower speed across the boundary in front of the wedge (see Figure 5.2). While this may be a result of the low speed used, it is clear that a larger grid could better capture the transition from free stream to flow around the wedge. A similar problem can be seen in both the pressure and velocity profiles on the top and bottom boundaries; as the shedding vortices approach the boundaries, they are forced to the free stream conditions. Both situations may be an artifact of the two dimensional nature of the model; having a third dimension will allow the flow to dissipate more quickly (as seen in the comparison of C_p values). When this study moves into the three dimensional realm, the need for widening the boundaries may be obviated.

Another area that would be worth additional study is the run-time parameters. The solutions shown here were generated using the default values for all the parameters (e.g. CFL, k and ω) and the SST turbulence model. It may be that some analysis of the model may show more appropriate values to use, or that a different turbulence model may be appropriate. *Wind* provides the option to combine SST with ‘Large Eddy Simulation’

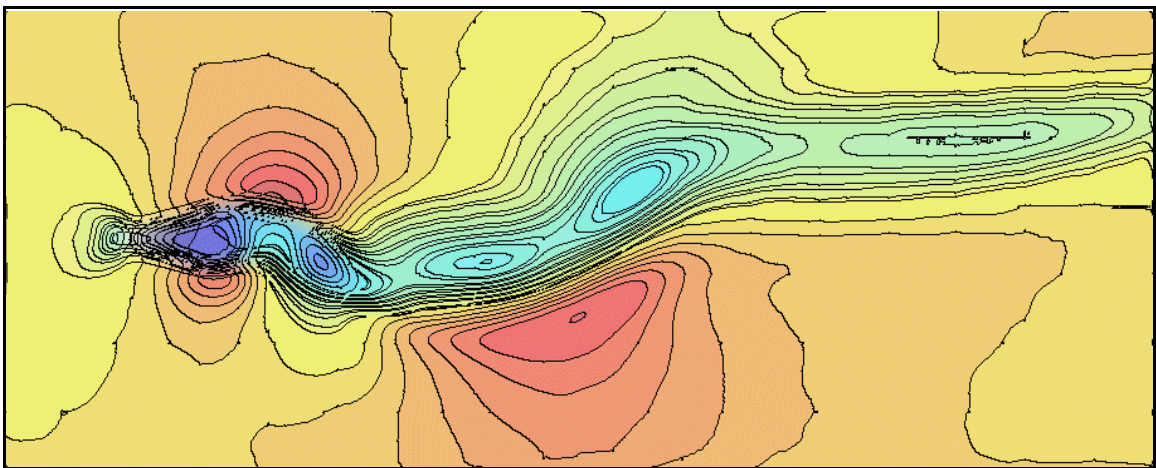


Figure 5.2 A contour plot of the average velocity. This sample for the 30° wedge run shows that the size of the grid used does have an impact on the solution. The leftmost edge is the inflow boundary and should be the free stream velocity across the entire length. In a similar manner, the top and bottom edges are free stream boundaries and can clearly be seen influencing the movement of the vortices downstream.

which can “...improve predictions of complex flows in a real-world engineering environment...” [8] and may provide better results than SST alone. On the other hand, SST may be more sophisticated than is needed for this simulation and a one-equation or algebraic model might achieve the same results with less processing requirements.

Eddy also studied the turbulence coupling effects of pairs of wedges [7] which could provide another point of comparison, as well as help determine how multiple wedges will interact. While the study of spanwise coupling will require a 3D model, streamwise coupling can be modeled by modifying the grid generation code to include two edges, one above the other (see Figure 5.3).

In order to produce values for comparison, the wedge geometry and testing conditions for this study were set to duplicate those in Eddy’s work. This fixed the wedge size and shape, as well as the free stream velocity, pressure and temperature. Since this study has shown that the modeling concept is sound, the next step should be to determine the requirements for the dynamic distortion generator wedge array. These should include specifications for the range of operating conditions, as well as any constraints that might influence the wedge design (e.g. the size of available actuators will affect the size of the wedge and its range of motion).

These recommendations are summarized in Table 5.1.

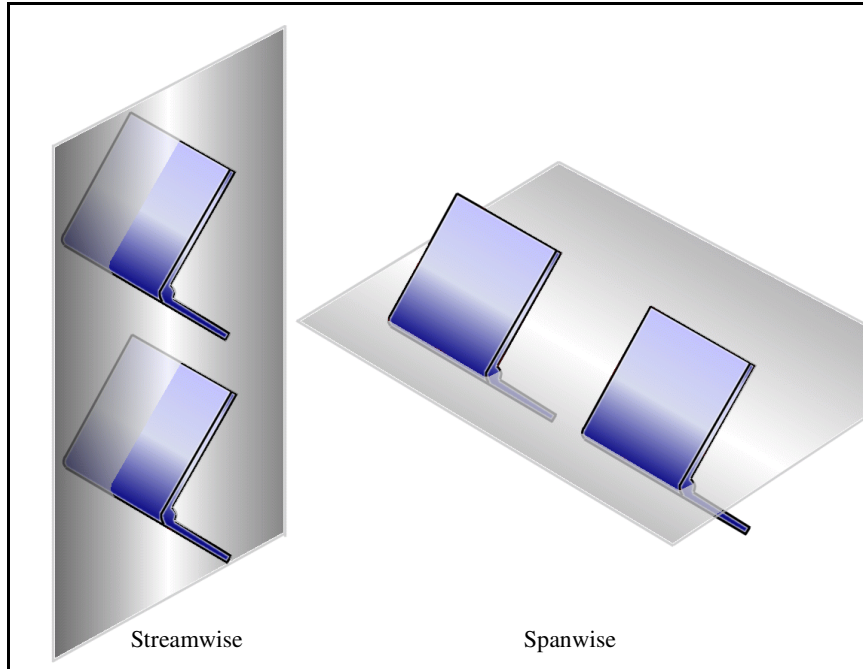


Figure 5.3 Sections needed to evaluate flow coupling for wedge pairs. These two dimensional sections will provide streamwise and spanwise flow coupling data for wedge pairs.

Table 5.1 Summary of recommendations for future work

Task	Purpose	Comment
Expand grid	Capture entire airflow	By adding at least one inch of grid to the upwind boundary, distortion across the boundary will be minimized. Expansion of the upper and lower boundaries will be helpful, but may not be necessary for the 3-D version and its increased dissipation.
Curve the grid at the wedge surface	Improve convergence	A “body fit” grid should achieve better results, especially in the wedge tip area where separation begins.
Switch to chimera	Simplify grid	A chimera based grid would require less zones and be easier to alter and may improve convergence for the same reasons as the curved grid suggested above.
Multiple wedges	Further verification, determine effects of coupling	The current two dimensional model could be modified to evaluate streamwise coupling effects by modeling two (or more) wedges mounted one over the other. This could be compared to the tests run by Eddy as well as demonstrating the coupling effects. (Spanwise coupling will require a 3D model.)
Evaluate turbulence models, parameters	Improve results, minimize run time	The keyword LESB may be used to combine the SST model with “Large Eddy Simulation” for selected zones and may improve the quality of results. Alternately, the Spalart one-equation model, combined with the DES (Detached Eddy Simulation) option may provide comparable solutions in less time.
Determine requirements	Ensure the correct problem is being solved	Determine the range of operating conditions that must be simulated, such as flow velocity, pressure and temperature, to make sure that the model can accommodate all the possible conditions.

References

List of References

- [1] Jumel, J., King, P.S., and O'Brien, W.F., "Transient Total Distortion Generator Development, Phase II," Final Technical Rept. F40600-94-K-0018, Arnold Engineering Development Center, Tullahoma, TN, July 1999.
- [2] Yang, J., Tsai, G., and Wang, W., "Near-Wake Characteristics of Various V-Shaped Bluff Bodies." *Journal of Propulsion and Power*, Vol. 10, No. 1, Jan.-Feb. 1994, pp. 47-55.
- [3] Parkinson, G.V. and Jandali, T., "A Wake Source Model for Bluff Body Potential Flow," *Journal of Fluid Mechanics*, Vol. 40, No. 3, 1970, pp.577-594.
- [4] Gerrard, J.H., *The Mechanics of the Formation Regions of Vortices Behind Bluff Bodies*," *Journal of Fluid Mechanics*, Vol. 25, No. 2, 1966, pp.401-413.
- [5] Bruns, J.E. and Smith, C.F., "Installed F/A-18 Inlet Flow Calculations at a High Angle of Attack," *Journal of Propulsion and Power*, Vol. 10, No. 1, Jan.-Feb. 1994, pp. 110-115.
- [6] Beale, D.K., "Improving Information Productivity and Quality in Turbine Engine Ground Testing," AIAA Paper 2001-0163, 2001.
- [7] Eddy, G.L. Jr., "Study of Steady State Wake Characteristics of Variable Angle Wedges," M.S. Dissertation, Virginia Polytechnic Institute and State University, Blacksburg, VA, 2001.
- [8] The NPARC Alliance, "WIND Users Guide,"
<http://www.grc.nasa.gov/WWW/wind/winddocs/user/user.pdf>.
- [9] Wilcox, D.C., *Turbulence Modeling for CFD*, DCW Industries, 1994, pp. 84-87.
- [10] White, F.M., *Fluid Mechanics*, WCB/McGraw-Hill, 1999, pp. 295-296.
- [11] White, F.M., *ibid*, pp. 427-430.

Appendices

A Grid Development

In spite of the simplicity of the model, care must be taken to arrive at a grid that will be adequately capture the behavior of the airflow. This must include an accurate representation of the wedge and a grid points that capture information within the boundary layer.

A.1 Wedge Geometry

The wedges used in Eddy's work were the basis of the model used in this study (see Figure A.1). These wedges started as stock steel door hinges which were trimmed to 1" long by 1.125" wide on each side of the 0.25" diameter hinge. These were then mounted on a 0.125" rod, replacing the hinge pin, that spanned the 12" by 12" wind tunnel. Set screws were mounted on the downwind side of the hinge to fix the angle for each test.

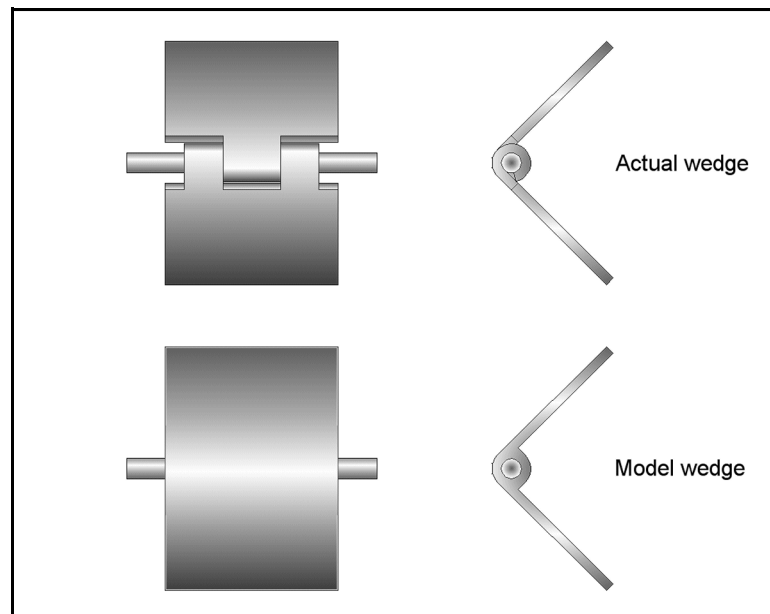


Figure A.1 The modified door hinge used by Eddy. The computer model wedge was simplified in the hinge area.

A.2 Wind Tunnel Test Section Geometry

The wind tunnel used in both the Jumel and Eddy studies pumps ambient air through honeycomb screens to smooth out turbulence before the nozzle accelerates the flow to 42 m/s in the 12" by 12" test section as seen in Figure A.2 [7]. The wedges are mounted on an eighth inch rod that spans the test section one inch upwind of the first measurement slot. A total of seven measurement slots allows for measurements from one to thirteen inches downwind of the wedge.

A.3 Boundary Layer Thickness

For the operating conditions of this study, a rough estimate of the Reynold's number was calculated using 42 m/s for the characteristic velocity, the 1 inch (0.0254 m) length of a single side of the hinge as a characteristic length, and STP value of 1.5×10^{-5} m²/s for the kinematic viscosity. A value of approximately 7×10^4 resulted, which suggested laminar flow and a worst case displacement thickness of approximately

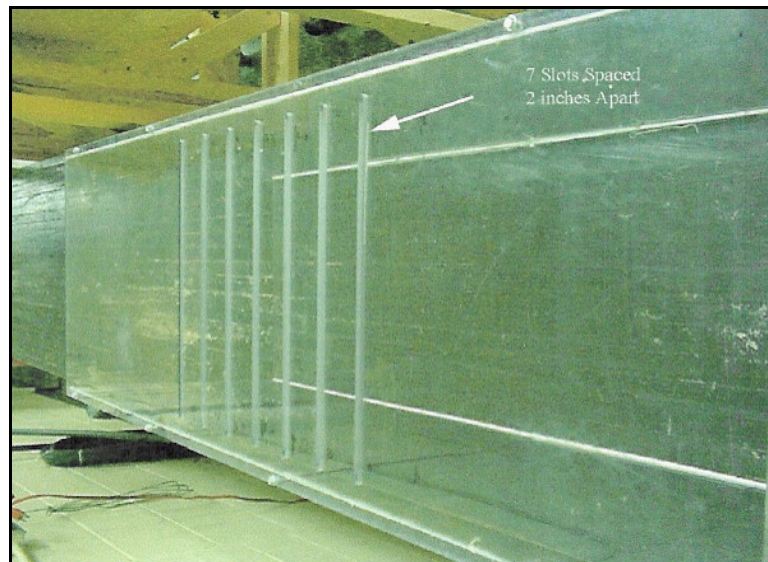


Figure A.2 The Lexan test section used in the Eddy study. The seven test slots are used for measuring pressure in cross section [7].

1.9x10⁻² inches, using the flat plate laminar flow formula seen in equation A.1 [11]. This calculation provides a value to base the minimum grid thickness at the wedge surface.

$$\frac{\delta}{x} \approx \frac{5.0}{\sqrt{Re_x}} \quad (\text{A.1})$$

A.4 Geometric Progression

In order to model the behavior of the airflow around the wedge, the grid must be fine enough to capture information within the boundary layer. However, making the entire grid that fine is wasteful as it is unnecessary. To compromise, a scheme is needed to reduce the grid size as the grid approaches the surface of the wedge. To accomplish this, a simple geometric series is used. This will reduce the grid in a consistent manner, as well as allowing for adjustments to be made without major coding changes. The series is described mathematically thus;

$$a+ar+ar^2+ar^3+\dots+ar^{n-1}=\frac{a(1-r^n)}{1-r}=\frac{a-l}{1-r} \quad (\text{A.2})$$

Where $l=ar^{n-1}$ and $r \neq 1$. The grid can now be defined by three different schemes. The first is a simple uniform spacing for the regions that are relatively distant from the surface. The second is a spacing that reduces from the fixed size to less than the boundary layer thickness. The third is the reverse of the second, growing from smaller than the boundary layer thickness to the fixed size. In programming terms, a maximum spacing is defined that corresponds to a , a minimum spacing l , and an arbitrary distance from the surface equals the sum. To simplify the coding, measurements are defined in terms of a unit length based on the length of a single “wing” of the wedge, and each of these schemes is set to half that length. The end result is that the sum works out to;

$$\delta_{\max} + \frac{1}{2} = \frac{\delta_{\max} - r \cdot \delta_{\min}}{1-r} \quad (\text{A.3})$$

Which, after solving for r , becomes;

$$r = \frac{1}{1 + 2\delta_{\max} - 2\delta_{\min}} \quad (\text{A.3})$$

The end result is a value for r that can be used to calculate progressively smaller grid spacing down to the specified minimum size. This way, all that is required to alter the grid spacing (for instance, when the free stream velocity is changed) is to change the maximum and/or minimum spacing values, then re-running the code.

A.5 Plot-3D Grid File Format

The user guide for *wind* provided sample Fortran code for a simple demonstration grid. MatLab's superior matrix manipulation made it a more practical solution for developing the more complex grid, but MatLab's I/O routines do not map exactly to Fortran's. After some reverse engineering, it was determined that files needed to be written in the following format;

- **Zone count:** [int size] [int number of zones] [int size] (*size* is four bytes per int or 4).
- **Zone sizes:** [int size] [int $zone_1(imax\ jmax), \dots, zone_n(imax\ jmax)$] [int size] (*size* is four bytes per int, two ints per zone, and n zones or $4*2*n$)
- **Zones 1 to n :** [int size] [float $x_{11}, x_{12}, \dots, x_{ij}$] [float $y_{11}, y_{12}, \dots, y_{ij}$] [int size] (*size* is four bytes per float, two floats per point, and i by j points or $4*2*i*j$)

The end result is a structured Cartesian grid in *Plot-3D* multi-zone, 2D, single precision, binary (or unformatted) file with no "blank" or "intout/xintout". This can be altered to 3D by adding $jmax$ values to the zone sizes, z values to the zones, and adjusting the *sizes* accordingly.

A.6 Other Concerns

The geometry of the wedge is such that the exposed hinge surface “shifts” from back to front as the wedge angle decreases. In other words, when the wedge is fully opened (i.e. $\theta=180^\circ$), the two flaps form the entire upwind surface, while the hinge is only exposed in the back, but when the hinge is closed ($\theta=0^\circ$), then the leading edge of the wedge is a half cylinder surface. In order to compensate for this in the grid, it is necessary to code for the number of points on the front and back of the hinge to vary as the wedge angle changes.

B Sample Code and Parameters

The following samples include the grid generating MatLab “m-file”, as well as some additional MatLab utilities and REXX scripts.

This study was executed almost entirely on a desktop PC; a 1.3 GHz AMD Duron processor, 384 MB RAM, running the Red Hat 7.3 distribution of Linux (2.4.18 kernel), MatLab Student Edition release 12 (MatLab version 6), and ObjectREXX version 2.0. *Wind* and its supporting utilities are described in detail in appendix C.

Note: REXX is a very common “procedures” (or “scripting” in *nix parlance) language on IBM mainframes and is also available in some form on very nearly every PC operating system. While it is not commonly used on Linux, it is powerful, flexible and easy to code. The decision to write these utilities in REXX was based on more pragmatic reasons; the author is fairly fluent in REXX so it was much more expedient to code utilities with it, rather than spend time learning a more common scripting language.

B.1 Generating the Grid (MatLab m-file)

The following is the MatLab m-file that creates and writes the structured Cartesian grid.

```
%== 10-zone grid builder, 2-D, V4 =====
%=====
clc; %== clear the command window
%=====
%== Note to self: =====
%==     MatLab matrix notation is done in R,C format, so x ===
%==     values correspond to rows and y values columns. =====
%=====
%== "Fixed" values =====
%=====
L         = 1;            %= length (of one butterfly "wing") [inches]
                        %= note: this fixes the units and dimensions
t         = 0.060;       %= thickness of "wing" [unitless]
r         = 0.125;       %= radius of hinge [unitless]
theta     = 090*(pi/180); %= angle of "wings" [rad]
filename  = '2d090.grid'; %= for later use...
phi       = (pi-theta)/2; %= useful angle [rad]
beta      = pi/2-phi;    %= angle on back of hinge
max       = 0.1;         %= largest/ fixed division [unitless]
min       = 0.001;      %= smallest division [unitless]
```

```

zones      = 10;          %= number of zones
%=====
%== Calculated values =====
%=====
dec        = 1/(1+2*max-2*min); %= geometric-prog. decrement
%=====
%== Base sections =====
%=====
A          = [0:max:0.5]; %= fixed width area
size_A     = numel(A);
B(1)      = 0;          %= start at 0
delta     = max;
i         = 1;          %= start adding to second
while B(i) < 0.5
    delta = delta*dec;
    i = i + 1;
    B(i) = B(i-1) + delta;
    if delta < min
        B(i) = 0.5;
    end %= if..then
end
size_B     = i;
for i = 1:size_B
    C(i) = 0.5 - B(size_B-i+1);
end
size_C     = size_B;

%== pick how many points go on which side of the hinge =====
if theta > 150*(pi/180) | theta < 30*(pi/180)
    bogus_angle;

elseif theta >= 120*(pi/180)
    fore = 2;
elseif theta >= 90*(pi/180)
    fore = 4;
elseif theta >= 60*(pi/180)
    fore = 6;
else
    fore = 8;
end %=if..elseif..elseif..else
aft      = 10-fore;
%== pick how many divisions on the wingtip =====
tip      = 10;

%== grids =====
%== zone 1 - ahead of wing =====
max1     = [(size_A + 2*(size_A-1) + size_B-1) ...
            (2*size_A + 2*(size_B-1) + fore)];
X1       = zeros(max1(1),max1(2));
Y1       = X1;
%== zone 2 - behind wing =====
max2     = [(size_C + 7*(size_A-1)) (2*size_A + 2*(size_B-1) + aft)];
X2       = zeros(max2(1),max2(2));
Y2       = X2;
%== zone 3 - below wing, upwind =====
max3     = [(size_A + 2*(size_A-1) + (size_B-1)) ...
            (size_C + 4*(size_A-1))];
X3       = zeros(max3(1),max3(2));

```

```

Y3          = X3;
%== zone 4 - above wing, upwind =====
max4        = max3;
X4          = X3;
Y4          = X4;
%== zone 5 - below wingtip =====
max5        = [(tip+1) ...
               (size_C + 4*(size_A-1))];
X5          = zeros(max5(1),max5(2));
Y5          = X5;
%== zone 6 - above wingtip =====
max6        = max5;
X6          = X5;
Y6          = X6;
%== zone 7 - below wing, downwind =====
max7        = [(size_C + 7*(size_A-1)) ...
               (size_C + 4*(size_A-1))];
X7          = zeros(max7(1),max7(2));
Y7          = X7;
%== zone 8 - above wing, downwind =====
max8        = max7;
X8          = X7;
Y8          = X8;
%== zone 9 - middle section == (inc~=0.0625) =====
max9        = [55 90];
X9          = zeros(max9(1),max9(2));
Y9          = X9;

%== zone 10 - downwind section == (inc~=0.125) =====
max0        = [57 57];
X0          = zeros(max0(1),max0(2));
Y0          = X0;

%=====
%== Baselines =====
%=====
%== baseline 1 - y-values for zones 3, 4 =====
baseline1 = [A (A(2:size_A)+0.5) (A(2:size_A)+1.0) (A(2:size_A)+1.5)
             (B(2:size_B)+2.0)]/2.5;
%== baseline 2 - y-values for zones 1, 2 (wing front/back) =
baseline2 = [C (A(2:size_A)+0.5)]/1;
%== baseline 3 - x-values for zones 1, 3, 4 =====
baseline3 = [A ...
             (A(2:size_A)+0.5) ...
             (A(2:size_A)+1.0) ...
             (B(2:size_B)+1.5) ...
             (C(2:size_C)+2.0) ...
             (A(2:size_A)+2.5) ...
             (A(2:size_A)+3.0) ...
             (A(2:size_A)+3.5) ...
             (A(2:size_A)+4.0) ...
             (A(2:size_A)+4.5) ...
             (A(2:size_A)+5.0) ...
             (A(2:size_A)+5.5)]';
%== baseline 4 - x-values for zone 2 =====
baseline4 = (baseline3(max1(1):numel(baseline3))-baseline3(max1(1)))/4;

```

```

%== baseline 5 - x-values for zones 5,6 =====
baseline5 = [0:(1/tip):1];
%== "origin" - x-y coords for center of rod =====
origin = [2 3.5];
%== "corner" - x-y coords for leading wingtip =====
corner = [origin(1)-r*cos(phi)+sin(phi) ...
          origin(2)-r*sin(phi)-cos(phi)];

%=====
%== Zone 1 - upwind of wing =====
%=====
X1(1,:) = 0;
Y1(1,:) = (2.5:2/(max1(2)-1):4.5);
X1(max1(1),1:(max1(2)-fore)/2) = [-baseline2*sin(phi)+corner(1)];
Y1(max1(1),1:(max1(2)-fore)/2) = [baseline2*cos(phi)+corner(2)];
for j = ((max1(2)-fore+2)/2):(max1(2)/2)
    k = j - (max1(2)-fore+2)/2 + 1;
    alpha = (fore+1-2*k)*phi/(fore+1);
    X1(max1(1),j) = (origin(1)-r*cos(alpha));
    Y1(max1(1),j) = (origin(2)-r*sin(alpha));
end %= for..j
%== fill it up =====
for j = 1:(max1(2)/2)
    opp = X1(max1(1),j)-X1(1,j);
    adj = Y1(max1(1),j)-Y1(1,j);
    hyp = sqrt(opp^2+adj^2);
    X1(1:max1(1),j) = X1(1,j) + opp*baseline3(1:max1(1))/2;
    X1(1:max1(1),(max1(2)+1-j)) = X1(1:max1(1),j);
    Y1(1:max1(1),j) = Y1(1,j) + adj*baseline3(1:max1(1))/2;
    Y1(1:max1(1),(max1(2)+1-j)) = 7-Y1(1:max1(1),j);
end %= for..j

%=====
%== Zone 2 - immediately downwind of wing =====
%=====
X2(max2(1),:) = 6;
Y2(max2(1),:) = (2.5:2/(max2(2)-1):4.5);
X2(1,1:(max2(2)-aft)/2) =
[-(1-r)*baseline2*sin(phi)+corner(1)+t*cos(phi)];
Y2(1,1:(max2(2)-aft)/2) =
[(1-r)*baseline2*cos(phi)+corner(2)+t*sin(phi)];
for j = ((max2(2)-aft+2)/2):(max2(2)/2)
    k = j - (max2(2)-aft+2)/2;
    alpha = (aft-1-2*k)*beta/(aft-1);
    X2(1,j) = (origin(1)+r*cos(alpha));
    Y2(1,j) = (origin(2)-r*sin(alpha));
end %= for..j
%== fill it up =====
for j = 1:(max2(2)/2)
    opp = X2(max2(1),j)-X2(1,j);
    adj = Y2(max2(1),j)-Y2(1,j);
    hyp = sqrt(opp^2+adj^2);
    X2(1:max2(1),j) = X2(1,j) + opp*baseline4;
    X2(1:max2(1),(max2(2)+1-j)) = X2(1:max2(1),j);
    Y2(1:max2(1),j) = Y2(1,j) + adj*baseline4;
    Y2(1:max2(1),(max2(2)+1-j)) = 7-Y2(1:max2(1),j);
end %= for..j

```

```

%=====
%== Zone 3,4 - below/above wing, upwind =====
%=====
X3(1,:) = 0;
Y3(1,:) = [0:(2.5/(max3(2)-1)):2.5];
X3(max3(1),:) = corner(1);
Y3(max3(1),:) = corner(2)*baseline1;
%== fill it up =====
for j = 1:max3(2)
    opp = X3(max3(1),j)-X3(1,j);
    adj = Y3(max3(1),j)-Y3(1,j);
    X3(:,j) = corner(1)*baseline3(1:max3(1))/2;
    X4(:,(max3(2)+1-j)) = X3(:,j);
    Y3(:,j) = Y3(1,j) + adj*baseline3(1:max1(1))/2;
    Y4(:,(max3(2)+1-j)) = 7-Y3(:,j);
end %== for..j

%=====
%== Zone 5,6 - below/above wingtip =====
%=====
X5(1,:) = X3(max3(1),:);
Y5(1,:) = Y3(max3(1),:);
X5(max5(1),:) = corner(1)+t*cos(phi);
Y5(max5(1),:) = (corner(2)+t*sin(phi))*baseline1;
%== fill it up =====
for j = 1:max5(2)
    opp = X5(max5(1),j)-X5(1,j);
    adj = Y5(max5(1),j)-Y5(1,j);
    X5(:,j) = [corner(1):(opp/tip):(corner(1)+t*cos(phi))]' ;
    X6(:,(max5(2)+1-j)) = X5(:,j);
    Y5(:,j) = Y5(1,j) + adj*baseline5';
    Y6(:,(max5(2)+1-j)) = 7-Y5(:,j);
end %== for..j

%=====
%== Zone 7,8 - below/above wing, downwind =====
%=====
X7(1,:) = X5(max5(1),:);
Y7(1,:) = Y5(max5(1),:);
X7(max7(1),:) = 6;
Y7(max7(1),:) = [0:(2.5/(max7(2)-1)):2.5];
%== fill it up =====
for j = 1:max7(2)
    opp = X7(max7(1),j)-X7(1,j);
    adj = Y7(max7(1),j)-Y7(1,j);
    X7(:,j) = X7(1,j)+opp*baseline4;
    X8(:,(max7(2)+1-j)) = X7(:,j);
    Y7(:,j) = Y7(1,j) + adj*baseline4;
    Y8(:,(max7(2)+1-j)) = 7-Y7(:,j);
end %== for..j

%=====
%== Zone 9 - downwind, close =====
%=====
X9(:,1) = [6:((10-6)/(max9(1)-1)):10]' ;
Y9(:,1) = 0;
Y9(1,:) = [0:((7-0)/(max9(2)-1)):7];
%== fill it up =====

```

```

for j = 2:max9(2)
    X9(:,j) = X9(:,1);
    Y9(:,j) = Y9(1,j);
end %== for..j

%=====
%== Zone 10 - downwind, far =====
%=====
X0(:,1) = [10:((17-10)/(max0(1)-1)):17]';
Y0(:,1) = 0;
Y0(1,:) = [0:((7-0)/(max0(2)-1)):7];
%== fill it up =====
for j = 2:max0(2)
    X0(:,j) = X0(:,1);
    Y0(:,j) = Y0(1,j);
end %== for..j

%== "resize" as needed =====
%== - this doesn't do anything now, since L=1 inch, but =====
%== this will make conversion easy (say, to cm or ft). =====
%== - OTOH, caution required since WIND uses the units =====
%== defined in GMAN which default to inches... =====
X1 = L*X1;
Y1 = L*Y1;
X2 = L*X2;
Y2 = L*Y2;
X3 = L*X3;
Y3 = L*Y3;
X4 = L*X4;
Y4 = L*Y4;
X5 = L*X5;
Y5 = L*Y5;
X6 = L*X6;
Y6 = L*Y6;
X7 = L*X7;
Y7 = L*Y7;
X8 = L*X8;
Y8 = L*Y8;
X9 = L*X9;
Y9 = L*Y9;
X0 = L*X0;
Y0 = L*Y0;

%== display that puppy =====
hold off;
surf(X1,Y1,zeros(max1(1),max1(2)),'facecolor',[0.6 0.6 0.6])
hold on;
surf(X2,Y2,zeros(max2(1),max2(2)),'facecolor',[1.0 0.6 0.6])
surf(X3,Y3,zeros(max3(1),max3(2)),'facecolor',[0.6 1.0 0.6])
surf(X4,Y4,zeros(max4(1),max4(2)),'facecolor',[0.6 1.0 0.6])
surf(X5,Y5,zeros(max5(1),max5(2)),'facecolor',[1.0 1.0 0.6])
surf(X6,Y6,zeros(max6(1),max6(2)),'facecolor',[0.6 1.0 1.0])
surf(X7,Y7,zeros(max7(1),max7(2)),'facecolor',[0.6 0.6 1.0])
surf(X8,Y8,zeros(max8(1),max8(2)),'facecolor',[0.6 0.6 1.0])
surf(X9,Y9,zeros(max9(1),max9(2)),'facecolor',[1.0 0.6 1.0])
surf(X0,Y0,zeros(max0(1),max0(2)),'facecolor',[0.6 1.0 1.0])
axis equal;
set(gca,'view',[0 90]);

```



```

set(gca,'XLim',[0 17]);
set(gca,'YLim',[0 7]);
hold off;

%== write it in Plot3D format =====
fileout = fopen(filename,'w');
%== first, write the number of zones =====
wrtzone = fwrite(fileout,[4 zones 4],'int');
%== then, write the (2) dimensions =====
dims = [max1 max2 max3 max4 max5 max6 max7 max8 max9 max0];
dimbytes = 4*numel(dims);
wrtdims = fwrite(fileout,[dimbytes dims dimbytes],'int');
%== finally, write the good stuff =====
%== - note that single precision floats are 4 bytes, just =====
%== like ints. =====
zbytes1 = 4*2*numel(X1);
wrtpref = fwrite(fileout,[zbytes1],'int');
wrtX = fwrite(fileout,X1,'float');
wrtY = fwrite(fileout,Y1,'float');
wrtsuff = fwrite(fileout,[zbytes1],'int');
zbytes2 = 4*2*numel(X2);
wrtpref = fwrite(fileout,[zbytes2],'int');
wrtX = fwrite(fileout,X2,'float');
wrtY = fwrite(fileout,Y2,'float');
wrtsuff = fwrite(fileout,[zbytes2],'int');
zbytes3 = 4*2*numel(X3);
wrtpref = fwrite(fileout,[zbytes3],'int');
wrtX = fwrite(fileout,X3,'float');
wrtY = fwrite(fileout,Y3,'float');
wrtsuff = fwrite(fileout,[zbytes3],'int');
zbytes4 = 4*2*numel(X4);
wrtpref = fwrite(fileout,[zbytes4],'int');
wrtX = fwrite(fileout,X4,'float');
wrtY = fwrite(fileout,Y4,'float');
wrtsuff = fwrite(fileout,[zbytes4],'int');
zbytes5 = 4*2*numel(X5);
wrtpref = fwrite(fileout,[zbytes5],'int');
wrtX = fwrite(fileout,X5,'float');
wrtY = fwrite(fileout,Y5,'float');
wrtsuff = fwrite(fileout,[zbytes5],'int');
zbytes6 = 4*2*numel(X6);
wrtpref = fwrite(fileout,[zbytes6],'int');
wrtX = fwrite(fileout,X6,'float');
wrtY = fwrite(fileout,Y6,'float');
wrtsuff = fwrite(fileout,[zbytes6],'int');
zbytes7 = 4*2*numel(X7);
wrtpref = fwrite(fileout,[zbytes7],'int');
wrtX = fwrite(fileout,X7,'float');
wrtY = fwrite(fileout,Y7,'float');
wrtsuff = fwrite(fileout,[zbytes7],'int');
zbytes8 = 4*2*numel(X8);
wrtpref = fwrite(fileout,[zbytes8],'int');
wrtX = fwrite(fileout,X8,'float');
wrtY = fwrite(fileout,Y8,'float');
wrtsuff = fwrite(fileout,[zbytes8],'int');
zbytes9 = 4*2*numel(X9);
wrtpref = fwrite(fileout,[zbytes9],'int');
wrtX = fwrite(fileout,X9,'float');

```

```

wrtY    = fwrite(fileout,Y9,'float');
wrtstuff = fwrite(fileout,[zbytes9],'int');
zbytes0 = 4*2*numel(X0);
wrtstuff = fwrite(fileout,[zbytes0],'int');
wrtX    = fwrite(fileout,X0,'float');
wrtY    = fwrite(fileout,Y0,'float');
wrtstuff = fwrite(fileout,[zbytes0],'int');
%== close the file =====
closeit = fclose(fileout);
%== all done... =====

```

B.2 Sample Run Parms (*wind* dat-file)

Wind requires a parameter file to execute. The following sample was used for one of the test runs;

```

2D, 90 degree flap, SST, M=0.125
/ Inlet conditions - mach, pressure, temp, attack, yaw
Freestream total 0.125 14.7 530.0 0.0 0.0

/ Boundary conditions - based on freestream
Downstream pressure freestream zone 10

/ Viscous terms - Shear Stress Transport 2 eqn model
Turbulence SST

/ Numerics - 5 iterations per cycle
Cycles 20

End

```

The first line(s) is a freeform title that is included in later output files. The “/” character indicates a comment. The “freestream” keyword is followed by “static” or “total”, then the Mach number of the freestream, the pressure (in psi), the temperature (in degrees Rankine), the angle of attack and then angle of yaw (in degrees). For these conditions, the Mach number of 0.125 translates to 42.5 m/s which is slightly higher than the maximum sustainable velocity of 42 m/s managed in the Eddy study’s wind tunnel. The “turbulence” keyword is followed by one of nine different turbulence models available in *wind*. In this case, the SST (Shear Stress Transport) two equation model was selected as most appropriate for the calculations being done (see section 3.3). The “cycles” keyword is used to specify the number of 5-iteration cycles to run. Selecting 20 cycles and running multiple times allowed the automation of “snapshots” of the solution as it developed.

B.3 Running Wind Multiple Times (REXX script)

In order to capture data as the solution evolved, it was necessary to run *wind* multiple times, stopping in between to “snapshot” the results. *Wind* is designed to default to continuing where it left off when interrupted, making this a straightforward set up. The parameters (see B.2) were set to 100 iterations (20 five-iteration cycles) to allow a reasonable number of calculations between each stop.

```
#!/usr/bin/rexx
/* run_many.cmd - REXX exec to execute WIND multiple times *****/
trace 'O'

/* read in the filename for .dat, .lis, .cfl files *****/
/* note: file_names ARE case sensitive. use "parse arg" instead... **/
parse arg angle suffix .
if \datatype(angle,'N') then do /* angle is not numeric; use default */
  file_name = '2d120'
  grid_name = '2d120'
end /* if..then..do */
else do
  angle      = right(angle,3,'0') /* force zero-padding, 3 digits ****/
  file_name = '2d'angle||suffix
  grid_name = '2d'angle
end /* else..do */

/* copy the grid file for use with CFPOST *****/
"cp" grid_name".cfd temp.cgd"

say "Executing wind for input file" file_name".dat"

/* 5 iterations per cycle, 20 cycles per run = 10000 iterations. ****/
do i = 1 to 100
  fu = i-1 /* just a "before" variable *****/
  say "==== Iteration" fu"01 to" i"00 =====" time()
  "wind -runinplace", /* force to run locally *****/
  "-runque REAL", /* run in the "real" queue *****/
  "-dat" file_name, /* specify the dat file *****/
  "-list" file_name,
  "-grid" grid_name,
  "-flow" file_name,
  "-program wind5", /* specify which version to run *****/
  "-batch", /* force batch (no prompting) *****/
  "-nobg" /* force foreground *****/

  /* Theoretically, rc is set to the exit return code from the */
  /* command issued. However, a bad grid file during a test run */
  /* demonstrated that WIND (or perhaps Linux commands in general) */
  /* does not set the rc properly; use "tail -f <filename.lis> to */
  /* ensure that things are running correctly... *****/
  if rc = 0 then do
    /* set up the flow-file for use with CFPOST *****/
    "cp" file_name".cfl temp.cfl"
```

```

    "cfpost < mkplot.jou >" file_name"."right(i,3,'0')".log"
    "cp temp.q" file_name"."right(i,3,'0')".q"
    "cp" file_name".cfl" file_name"."right(i,3,'0')".cfl"
end /* if..then..do */
else do
    say "*** failed around" i"00 iterations with rc="rc
    leave
end /* else..do */
end /* do..i */

exit

```

B.4 Pressure and Velocity Data Extraction (REXX script)

The *cfpost* utility provides the facility to extract different data from the “common flow file” generated by *wind*. With the right supporting software (e.g. *Visual3*), this data can be displayed directly from *cfpost*. As an alternative, data can be extracted as space-delimited text for processing less directly; this utility executes a script in *cfpost* that does just that, for each “snapshot” taken during the *wind* run.

```

#!/usr/bin/rexx
/* smee.cmd - REXX kludge to generate output for "clean_list.cmd" */
trace 'O'

/* read in the filename for .dat, .lis, .cfl files *****/
/* note: file_names ARE case sensitive. use "parse arg" instead... */
parse arg angle suffix .
if \datatype(angle,'N') then do /* if angle is not numeric, default */
    file_name = '2d120'
    grid_name = '2d120'
end /* if..then..do */
else do
    angle      = right(angle,3,'0') /* force zero-padding, 3 digits ****/
    file_name  = '2d'angle||suffix
    grid_name  = '2d'angle
end /* else..do */

/* copy the grid file for use with CFPOST *****/
"cp" grid_name".cgd temp.cgd"

/* set up the flow-file for use with CFPOST *****/
do i = 1 to 100
    "cp" file_name"."right(i,3,'0')".cfl temp.cfl"
    "cfpost < p_plot.jou > p_plot.log"
    "cfpost < v_plot.jou > v_plot.log"
    "clean_list.cmd >"file_name"."right(i,3,'0')".csv"
end /* do..i */

exit

```

B.5 Clean-up Cfpst Output (REXX script)

The output from the previous step is not easily readable with any of MatLab's standard routines, so another utility was written to strip headers and extra spaces from the output and add commas between values. This allows the results to be read directly in to MatLab with a CSVREAD (Comma Separated Values read) routine.

```
#!/usr/bin/rexx
/* REXX exec to clean up output from CFPOST *****/
trace 'N'

/* set a signal ("goto") to close files after interupt *****/
signal on halt

/* identify files with pressure and velocity values *****/
file1 = "p_temp.lis"
file2 = "v_temp.lis"

/* open output files from CFPOST *****/
void = stream(file1,"C","OPEN")
void = stream(file2,"C","OPEN")
curzone = 0

/* read through the output files which should be the same length...*/
do while lines(file1) > 0
  /* parse around the "ZONE" header: if it's there, then get the */
  /* zone dimensions, otherwise build the output string which will */
  /* include i, j, k, x, y, p. p0, v, u, V and W *****/
  parse upper value linein(file1) with before "ZONE" after .
  parse upper value linein(file2) with . . . v_data
  if datatype(after,"N") then do /* ignore non-numeric "zones" *****/
    if after > 0 & curzone \= after then do
      if curzone > 0 then
        call write_zone
      else
        nop
      curzone = after
      big_i = 0
      big_j = 0
      big_k = 0
    end /* if..do */
  else
    nop
  end /* if..do */
  else do /* "ZONE" not found, but is it data or header? *****/
    parse var before i j k p_data
    if \datatype(i,"N") then /* if i is not numeric, then skip it */
      iterate
    else do /* step up the max i, j, k values to find dimensions *****/
      if big_i < i then
        big_i = i
    end
  end
end
```

```

    if big_j < j then
        big_j = j
    if big_k < k then
        big_k = k
    /* it's a data line: parse out the desired values *****/
    parse var p_data x y p p0 .
    p_data = x','y','p','p0 /* we need commas for CSVREAD to work */
    parse var v_data u v big_V big_W .
    v_data = u','v','big_V','big_W
    queue i','j','k','p_data','v_data /* "stack" the output rec ***/
end /* else..do */
end /* else..do */
end /* do..while */

call write_zone /* the very last zone is still in the stack *****/

/* interrupted or finished; close the input files *****/
halt:
void = stream(file1,"C","CLOSE")
void = stream(file2,"C","CLOSE")

exit

write_zone: /*****/
/*****/
/* this subroutine pulls a single zone's info off the stack and */
/* writes it to STDOUT. When everything works, just use the ">" */
/* redirection operator to pipe the output to a file... */
/*****/
    say big_i','big_j','big_k /* write the zone dimensions *****/
do queued()
    pull stuff
    say stuff
end /* do..queued() */
return

```

B.6 Displaying “Surfaces” (MatLab m-file)

The previous two utilities result in a file with data (static and total pressure, velocity in x and y and an average, and vorticity in this case, though other data can be extracted) in an array that can be read into arrays for each zone and then displayed with the following code and, optionally, saved in different formats. There is a lot of redundancy in the code, but the arrays vary in size from zone to zone, and zones 1 and 2 vary in size for different wedge angles.

```

%== Kludge to show pressure "surfaces" =====
%==+====1====+====2====+====3====+====4====+====5====+====6====+====7
clc;

clear X1 X2 Y1 Y2 P1 P2 V1 V2 fu1 fu2;

```

```

clem = '2d090.100.csv';
p_jpeg = '2d090.p.100.jpeg';
v_jpeg = '2d090.v.100.jpeg';
j_flag = 0;
WoT = csvread(clem);
WoT(:,8) = WoT(:,8)/12; %== convert in/s to f/s =====
WoT(:,9) = WoT(:,9)/12; %== convert in/s to f/s =====
WoT(:,10) = WoT(:,10)/12; %== convert in/s to f/s =====
WoT(:,11) = WoT(:,11)/12; %== convert in/s to f/s =====
p_max = 14.8;
WoT(:,6) = ((p_max - WoT(:,7))/p_max)*100;

bar = 6; %== metasyntactic var to select values =====
%== 6: p (static pressure [psi]) =====
%== 7: p0 (total pressure [psi]) =====
%== 8: u (x-velocity [ft/s]) =====
%== 9: v (y-velocity [ft/s]) =====
%== 10: V ( average velocity [ft/s]) =====
%== 11: W ( average vorticity [??]) =====
color_limits = [[0 3]; ... %== for pressure [psi] =====
[14.2 14.9]; ... %== for total pressure [psi] =====
[-250.0 250.0]; ... %== for x-velocities [ft/s] =====
[-150.0 150.0]; ... %== for y-velocities [ft/s] =====
[0.0 200.0]; ... %== for average velocity [ft/s] =====
[0.0 500.0]]; .. %== for average vorticity [ft/s] =====

count = 1;
%== zone 1 =====
imax = WoT(count,1);
jmax = WoT(count,2);
kmax = WoT(count,3);
X1 = zeros(imax, jmax);
Y1 = zeros(imax, jmax);
ful = zeros(imax, jmax);
entries = imax*jmax*kmax;

for l = 1:entries;
count = count + 1;
i = WoT(count,1);
j = WoT(count,2);
x = WoT(count,4);
y = WoT(count,5);
P_0 = WoT(count,7);
V = WoT(count,10);
fu = WoT(count,bar);
X1(i,j) = x;
Y1(i,j) = y;
P1(i,j) = P_0;
V1(i,j) = V;
ful(i,j) = fu;
end
count = count + 1;

%== zone 2 =====
imax = WoT(count,1);
jmax = WoT(count,2);

```

```

kmax = WoT(count,3);
X2 = zeros(imax, jmax);
Y2 = zeros(imax, jmax);
fu2 = zeros(imax, jmax);
entries = imax*jmax*kmax;
for l = 1:entries;
    count = count + 1;
    i = WoT(count,1);
    j = WoT(count,2);
    x = WoT(count,4);
    y = WoT(count,5);
    P_0 = WoT(count,7);
    V = WoT(count,10);
    fu = WoT(count,bar);
    X2(i,j) = x;
    Y2(i,j) = y;
    P2(i,j) = P_0;
    V2(i,j) = V;
    fu2(i,j) = fu;
end
count = count + 1;

%== zone 3 =====
imax = WoT(count,1);
jmax = WoT(count,2);
kmax = WoT(count,3);
X3 = zeros(imax, jmax);
Y3 = zeros(imax, jmax);
fu3 = zeros(imax, jmax);
entries = imax*jmax*kmax;
for l = 1:entries;
    count = count + 1;
    i = WoT(count,1);
    j = WoT(count,2);
    x = WoT(count,4);
    y = WoT(count,5);
    P_0 = WoT(count,7);
    V = WoT(count,10);
    fu = WoT(count,bar);
    X3(i,j) = x;
    Y3(i,j) = y;
    P3(i,j) = P_0;
    V3(i,j) = V;
    fu3(i,j) = fu;
end

count = count + 1;
%== zone 4 =====
imax = WoT(count,1);
jmax = WoT(count,2);
kmax = WoT(count,3);
X4 = zeros(imax, jmax);
Y4 = zeros(imax, jmax);
fu4 = zeros(imax, jmax);
entries = imax*jmax*kmax;
for l = 1:entries;
    count = count + 1;
    i = WoT(count,1);

```



```

        j = WoT(count,2);
        x = WoT(count,4);
        y = WoT(count,5);
        P_0 = WoT(count,7);
        V = WoT(count,10);
        fu = WoT(count,bar);
        X4(i,j) = x;
        Y4(i,j) = y;
        P4(i,j) = P_0;
        V4(i,j) = V;
        fu4(i,j) = fu;
    end
    count = count + 1;

%== zone 5 =====
imax = WoT(count,1);
jmax = WoT(count,2);
kmax = WoT(count,3);
X5 = zeros(imax, jmax);
Y5 = zeros(imax, jmax);
fu5 = zeros(imax, jmax);
entries = imax*jmax*kmax;
for l = 1:entries;
    count = count + 1;
    i = WoT(count,1);
    j = WoT(count,2);
    x = WoT(count,4);
    y = WoT(count,5);
    P_0 = WoT(count,7);
    V = WoT(count,10);
    fu = WoT(count,bar);
    X5(i,j) = x;
    Y5(i,j) = y;
    P5(i,j) = P_0;
    V5(i,j) = V;
    fu5(i,j) = fu;
end
count = count + 1;

%== zone 6 =====
imax = WoT(count,1);
jmax = WoT(count,2);
kmax = WoT(count,3);
X6 = zeros(imax, jmax);
Y6 = zeros(imax, jmax);
fu6 = zeros(imax, jmax);
entries = imax*jmax*kmax;
for l = 1:entries;
    count = count + 1;
    i = WoT(count,1);
    j = WoT(count,2);
    x = WoT(count,4);
    y = WoT(count,5);
    P_0 = WoT(count,7);
    V = WoT(count,10);
    fu = WoT(count,bar);
    X6(i,j) = x;
    Y6(i,j) = y;

```

```

        P6(i,j) = P_0;
        V6(i,j) = V;
        fu6(i,j) = fu;
    end
    count = count + 1;

%== zone 7 =====
imax = WoT(count,1);
jmax = WoT(count,2);
kmax = WoT(count,3);
X7 = zeros(imax, jmax);
Y7 = zeros(imax, jmax);
fu7 = zeros(imax, jmax);
entries = imax*jmax*kmax;
for l = 1:entries;
    count = count + 1;
    i = WoT(count,1);
    j = WoT(count,2);
    x = WoT(count,4);
    y = WoT(count,5);
    P_0 = WoT(count,7);
    V = WoT(count,10);
    fu = WoT(count,bar);
    X7(i,j) = x;
    Y7(i,j) = y;
    P7(i,j) = P_0;
    V7(i,j) = V;
    fu7(i,j) = fu;
end
count = count + 1;

%== zone 8 =====
imax = WoT(count,1);
jmax = WoT(count,2);
kmax = WoT(count,3);
X8 = zeros(imax, jmax);
Y8 = zeros(imax, jmax);
fu8 = zeros(imax, jmax);
entries = imax*jmax*kmax;
for l = 1:entries;
    count = count + 1;
    i = WoT(count,1);
    j = WoT(count,2);
    x = WoT(count,4);
    y = WoT(count,5);
    P_0 = WoT(count,7);
    V = WoT(count,10);
    fu = WoT(count,bar);
    X8(i,j) = x;
    Y8(i,j) = y;
    P8(i,j) = P_0;
    V8(i,j) = V;
    fu8(i,j) = fu;
end
count = count + 1;

%== zone 9 =====
imax = WoT(count,1);

```

```

jmax = WoT(count,2);
kmax = WoT(count,3);
X9 = zeros(imax, jmax);
Y9 = zeros(imax, jmax);
fu9 = zeros(imax, jmax);
entries = imax*jmax*kmax;
for l = 1:entries;
    count = count + 1;
    i = WoT(count,1);
    j = WoT(count,2);
    x = WoT(count,4);
    y = WoT(count,5);
    P_0 = WoT(count,7);
    V = WoT(count,10);
    fu = WoT(count,bar);
    X9(i,j) = x;
    Y9(i,j) = y;
    P9(i,j) = P_0;
    V9(i,j) = V;
    fu9(i,j) = fu;
end
count = count + 1;

%== zone 10 =====
imax = WoT(count,1);
jmax = WoT(count,2);
kmax = WoT(count,3);
X0 = zeros(imax, jmax);
Y0 = zeros(imax, jmax);
fu0 = zeros(imax, jmax);
entries = imax*jmax*kmax;
for l = 1:entries;
    count = count + 1;
    i = WoT(count,1);
    j = WoT(count,2);
    x = WoT(count,4);
    y = WoT(count,5);
    P_0 = WoT(count,7);
    V = WoT(count,10);
    fu = WoT(count,bar);
    X0(i,j) = x;
    Y0(i,j) = y;
    P0(i,j) = P_0;
    V0(i,j) = V;
    fu0(i,j) = fu;
end

%== display that puppy =====
figure(1);
hold off;
surf(X1,Y1,fu1,'lines','none')
hold on;
surf(X2,Y2,fu2,'lines','none')
surf(X3,Y3,fu3,'lines','none')
surf(X4,Y4,fu4,'lines','none')
surf(X5,Y5,fu5,'lines','none')
surf(X6,Y6,fu6,'lines','none')
surf(X7,Y7,fu7,'lines','none')

```

```

surf(X8,Y8,fu8,'lines','none')
surf(X9,Y9,fu9,'lines','none')
surf(X0,Y0,fu0,'lines','none')
axis equal;
set(gca,'view',[0 90]);
set(gca,'XLim',[0 17]);
set(gca,'YLim',[0 7]);
set(gca,'CLim',color_limits((bar-5),:));
colorbar('horiz');
set(gca,'Color',[0.4 0.4 0.4])
set(gca,'Layer','top')
set(gca,'Xtick',[0:1:17])
set(gca,'XtickLabel',[0.0:1:17.0])
title('Other','fontsize',36);
hold off;

```

```

figure(2);
hold off;
surf(X1,Y1,P1,'lines','none')
hold on;
surf(X2,Y2,P2,'lines','none')
surf(X3,Y3,P3,'lines','none')
surf(X4,Y4,P4,'lines','none')
surf(X5,Y5,P5,'lines','none')
surf(X6,Y6,P6,'lines','none')
surf(X7,Y7,P7,'lines','none')
surf(X8,Y8,P8,'lines','none')
surf(X9,Y9,P9,'lines','none')
surf(X0,Y0,P0,'lines','none')
axis equal;
set(gca,'view',[0 90]);
set(gca,'XLim',[0 17]);
set(gca,'YLim',[0 7]);
set(gca,'CLim',color_limits(2,:));
colorbar('horiz');
set(gca,'Color',[0.4 0.4 0.4])
set(gca,'Layer','top')
set(gca,'Xtick',[0:1:17])
set(gca,'XtickLabel',[0.0:1:17.0])
title('Total Pressure','fontsize',36);
hold off;

```

```

if j_flag == 1
    saveas(gcf,p_jpeg);
    exit;
end %= if..then

```

```

figure(3);
hold off;
surf(X1,Y1,V1,'lines','none')
hold on;
surf(X2,Y2,V2,'lines','none')
surf(X3,Y3,V3,'lines','none')
surf(X4,Y4,V4,'lines','none')
surf(X5,Y5,V5,'lines','none')
surf(X6,Y6,V6,'lines','none')
surf(X7,Y7,V7,'lines','none')
surf(X8,Y8,V8,'lines','none')

```

```
surf(X9,Y9,V9,'lines','none')
surf(X0,Y0,V0,'lines','none')
axis equal;
set(gca,'view',[0 90]);
set(gca,'XLim',[0 17]);
set(gca,'YLim',[0 7]);
set(gca,'CLim',color_limits(5,:));
colorbar('horiz');
set(gca,'Color',[0.4 0.4 0.4])
set(gca,'Layer','top')
set(gca,'Xtick',[0:1:17])
set(gca,'XtickLabel',[0.0:1:17.0])
title('Average Velocity','fontsize',36);
hold off;

if j_flag == 2
    saveas(gcf,v_jpeg);
    exit;
end %= if..then
```

C Tools

Wind comes with a small suite of tools that provide for both pre- and post-processing.

C.1 *Cfcnvt* (version 1.45)

Ultimately, *wind* requires that input grid files be in what it calls “common grid format”. The utility *cfcnvt* is provided to (among other things) convert from popular grid formats to the common grid format required. For this study, grids were generated in *Plot-3D* format and then converted using this utility. Many other format conversions are available.

C.2 *Gman* (version 6.153)

Before *wind* can use a common grid formatted file, the boundary conditions must be defined for each zone within the grid. The *gman* utility is used to couple zones with shared boundaries, define external and uncoupled boundaries as walls, free-stream, inflow, etc., and even cut “holes” within a grid so chimeras can be coupled to the main grid. Various test options can be invoked to determine that all boundaries are defined, connected, and valid. A graphics mode is available to help development, while processing can be automated with scripts once the process is established.

C.3 *Wind* (version 5.193)

Wind is a very flexible “computational platform which may be used to numerically solve various sets of equations governing physical phenomena” [8]. In this study, *wind* provides the ability to model the airflow around a wedge in a free stream. It takes grid and parameter files as input and generates a “common flow file” of solution

data, as well as convergence data (either displayed on screen or written to a text file). The outputs are then used with post-processing tools for analysis.

C.4 *Resplt* (version unknown)

While executing, *wind* generates a list of residual data values for each iteration and zone. Once the run has ended, *resplt* can be used to extract the residual data and then save the data in a format that *cfpost* can display as a plot of log(residual) vs. iteration for the run.

C.5 *Cfpost* (version 3.163)

The utility *cfpost* provides a number of post-processing functions. It can be used to display residual plot data generated by *resplt*, as well as save those plots in various formats. It can also generate (in space delimited text form) lists of data for the grid points for analysis or further processing. It can generate *Plot-3D* formatted solution files that can be viewed with appropriate tools, such as *TecPlot*.

D Results

Overall, the results obtained encouraging. After settling down, the pressure and velocity plots showed the vortex shedding typical of bluff bodies. The values calculated were qualitatively similar to sample results extracted from the Eddy study.

Note: the pressure coefficient measurements were calculated using the following equation;

$$C_p = \left(\frac{P_{\max} - P}{P_{\max}} \right) \cdot 100\% \quad \text{(D.1)}$$

D.1 Solution and Convergence, 30° Wedge

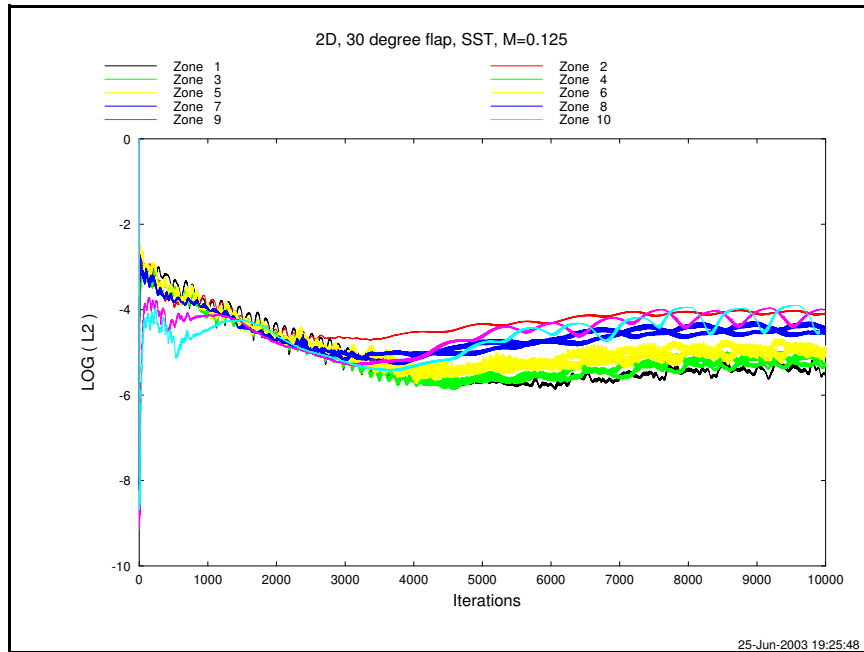


Figure D.1.1 Convergence data for *Navier-Stokes* calculations for the 30° wedge run.

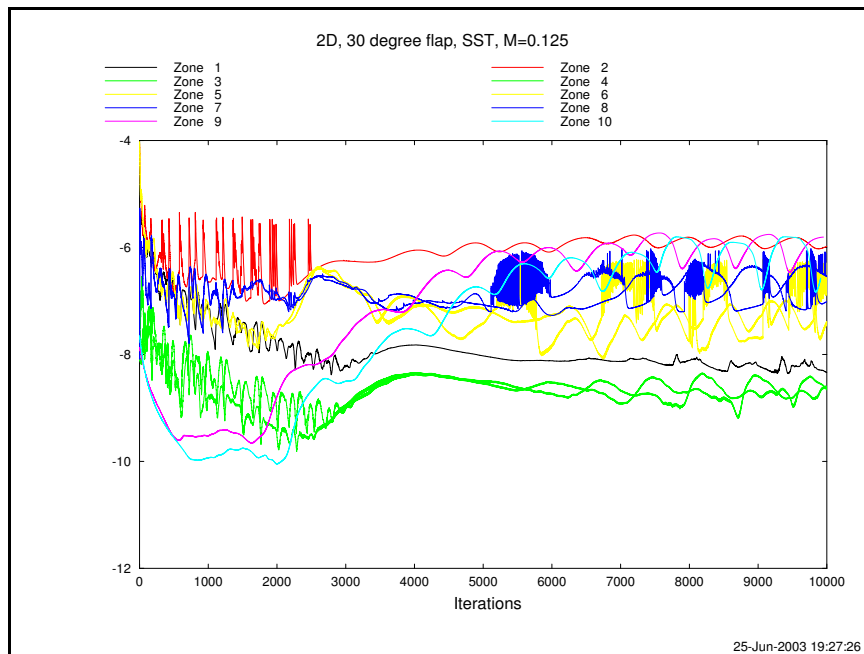


Figure D.1.2 Convergence data for *Shear Stress Transport* calculations, 30° wedge run.

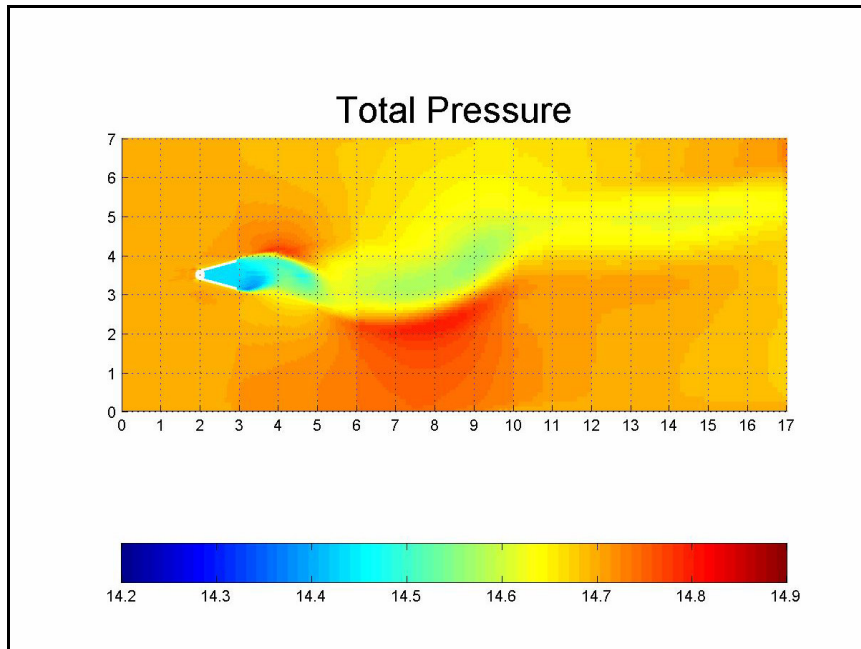


Figure D.1.3 Total pressure values for 30° wedge after 10,000 iterations.

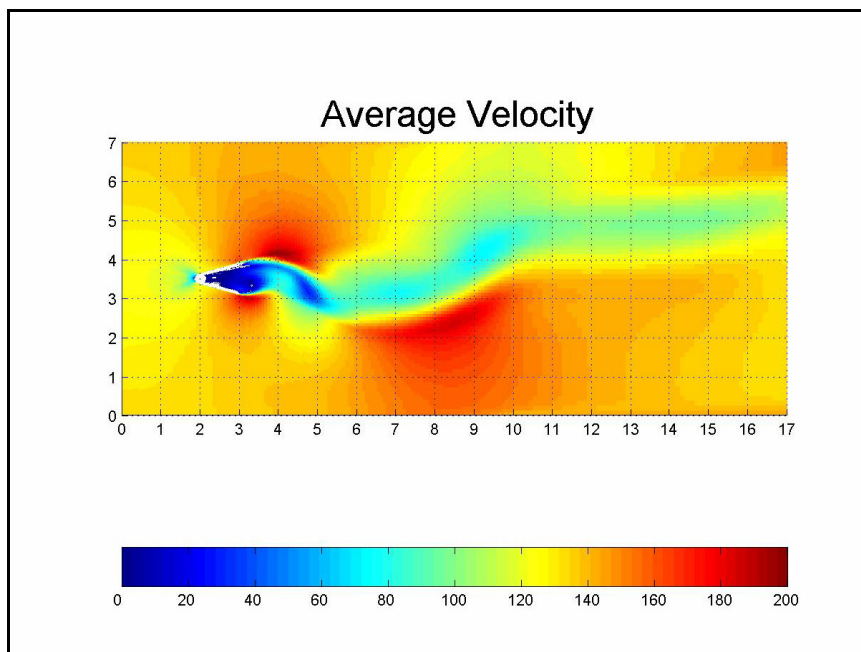


Figure D.1.4 Average velocity values for 30° wedge after 10,000 iterations.

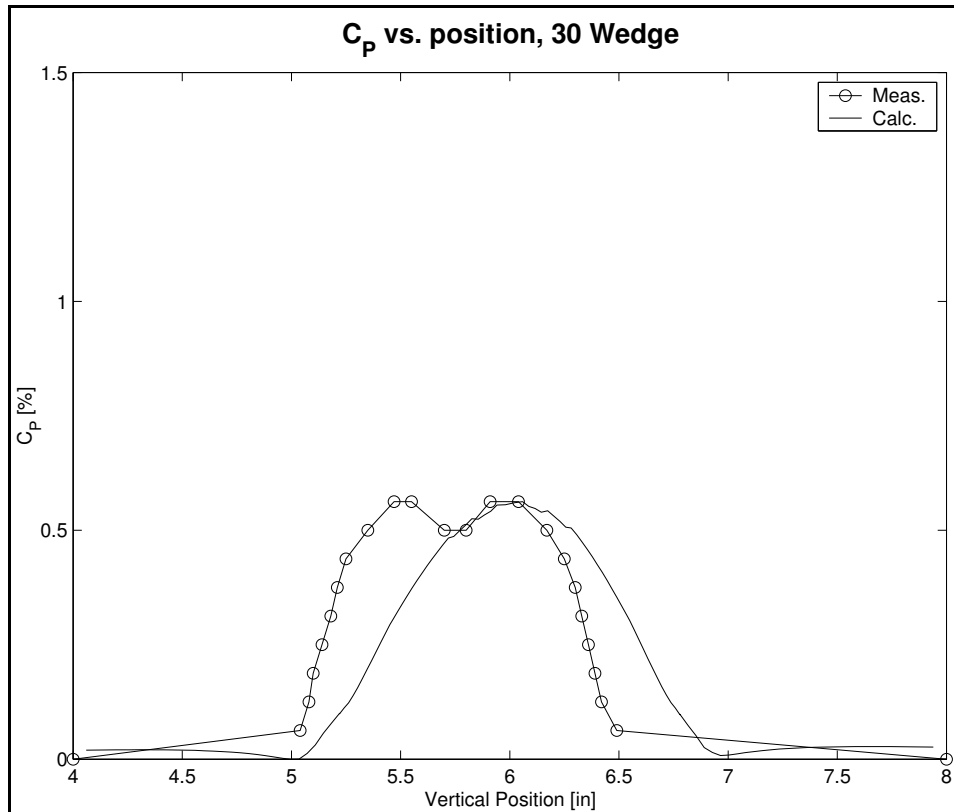


Figure D.1.5 Comparison of pressure coefficient data for 30° wedge. Values were measured at slot two (three inches downwind of the wedge) in the Eddy study and computed by *wind*. The calculated values are the average of three thousand iterations, normalized to the largest measured value of C_p due to the lack of measured maximum pressure data.

D.2 Solution and Convergence, 60° Wedge

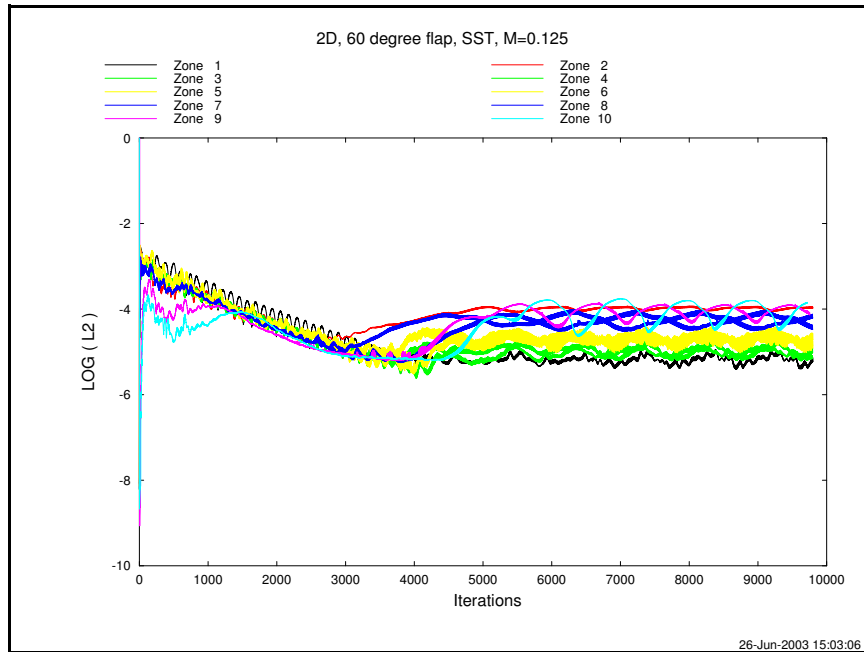


Figure D.2.1 Convergence data for *Navier-Stokes* calculations for the 60° wedge run.

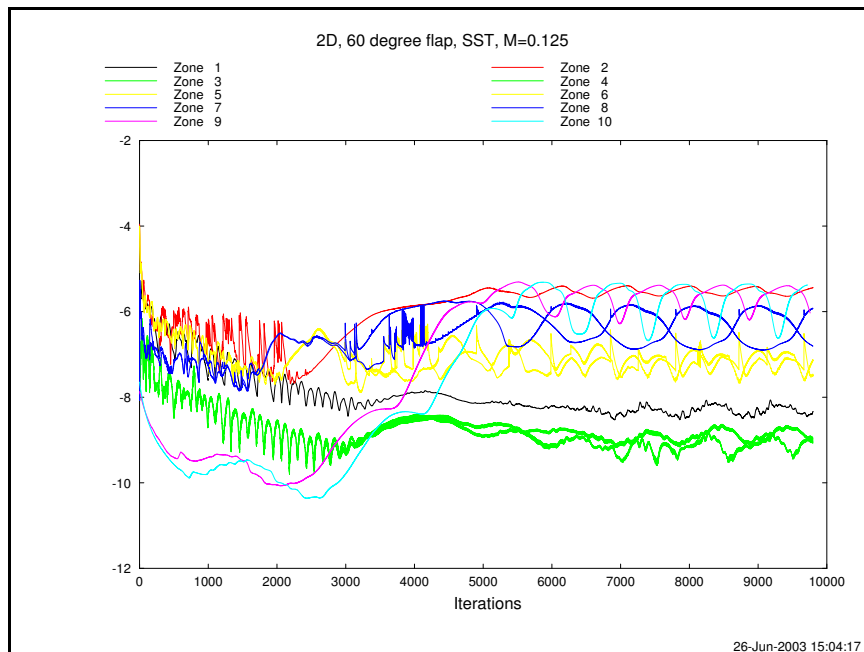


Figure D.2.2 Convergence data for *Shear Stress Transport* calculations, 60° wedge run.

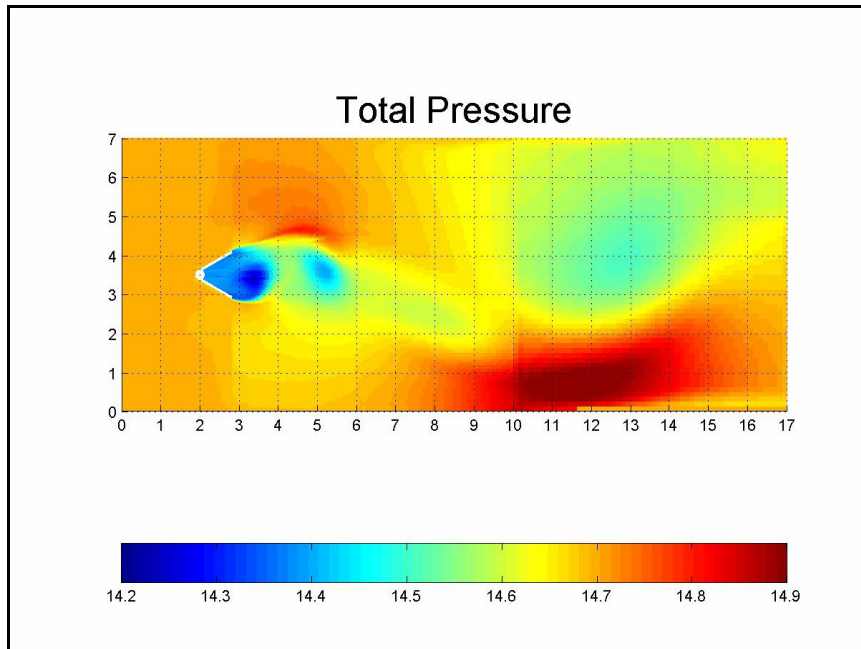


Figure D.2.3 Total pressure values for 60° wedge after 10,000 iterations.

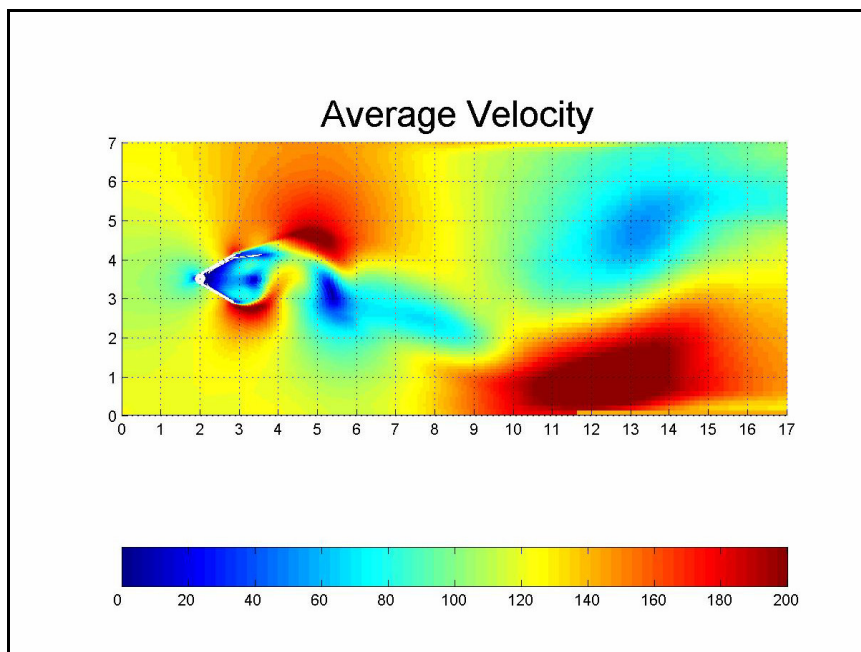


Figure D.2.4 Average velocity values for 60° wedge after 10,000 iterations.

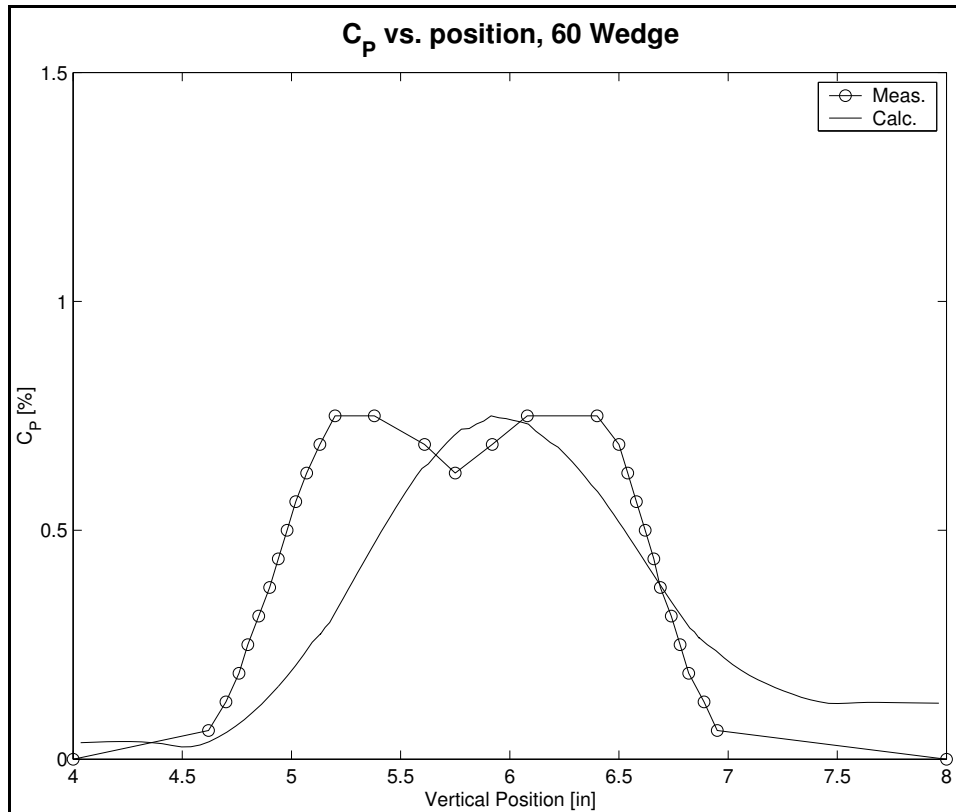


Figure D.2.5 Comparison of pressure coefficient data for 60° wedge. Values were measured at slot two (three inches downwind of the wedge) in the Eddy study and computed by *wind*. The calculated values are the average of three thousand iterations, normalized to the largest measured value of C_p due to the lack of measured maximum pressure data.

D.3 Solution and Convergence, 90° Wedge

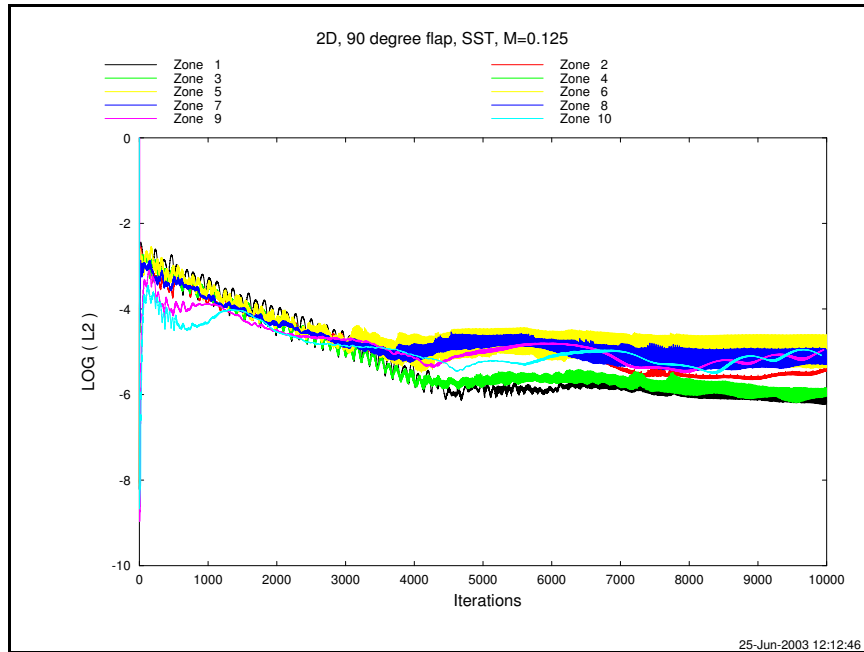


Figure D.3.1 Convergence data for *Navier-Stokes* calculations for the 90° wedge run.

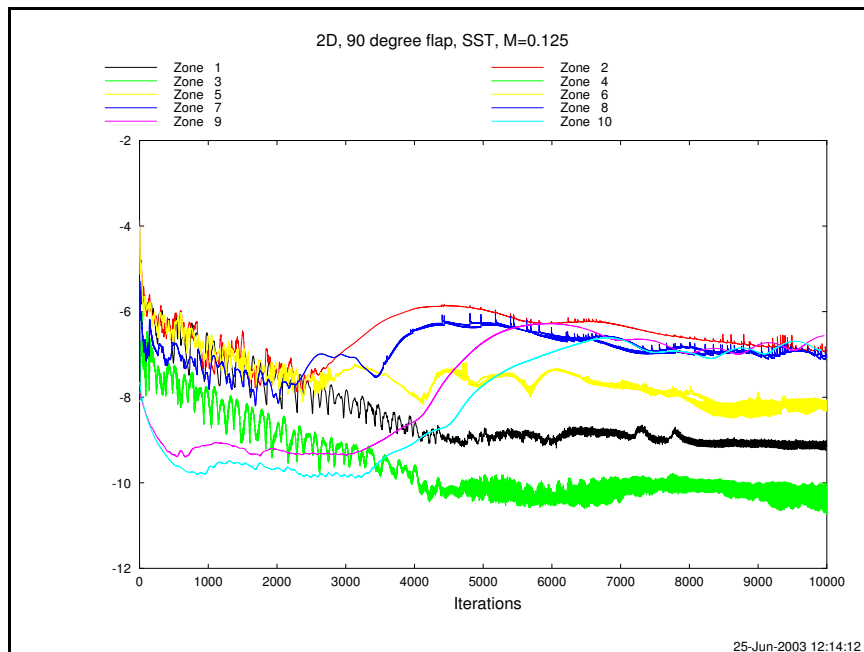


Figure D.3.2 Convergence data for *Shear Stress Transport* calculations, 90° wedge run.

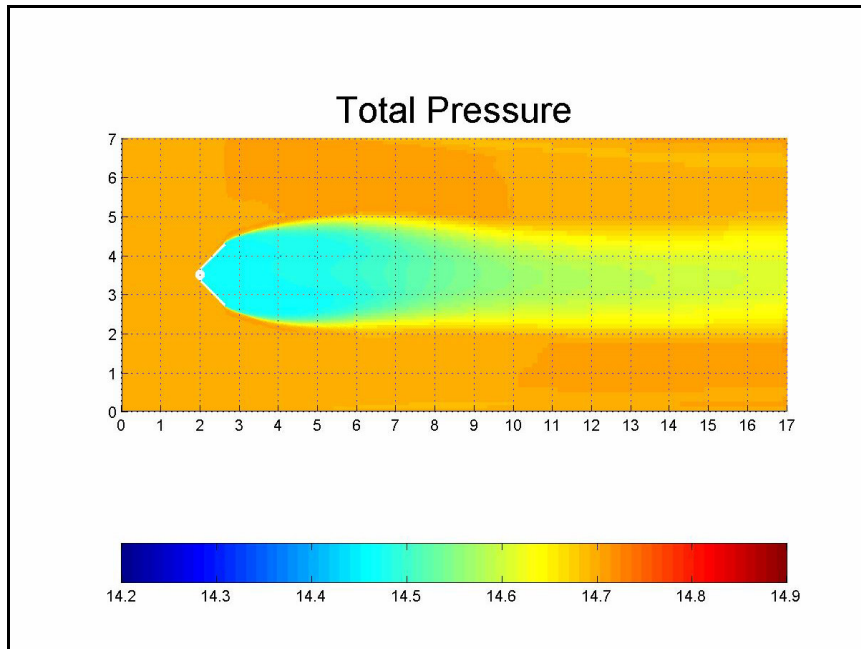


Figure D.3.3 Total pressure values for 90° wedge after 10,000 iterations.

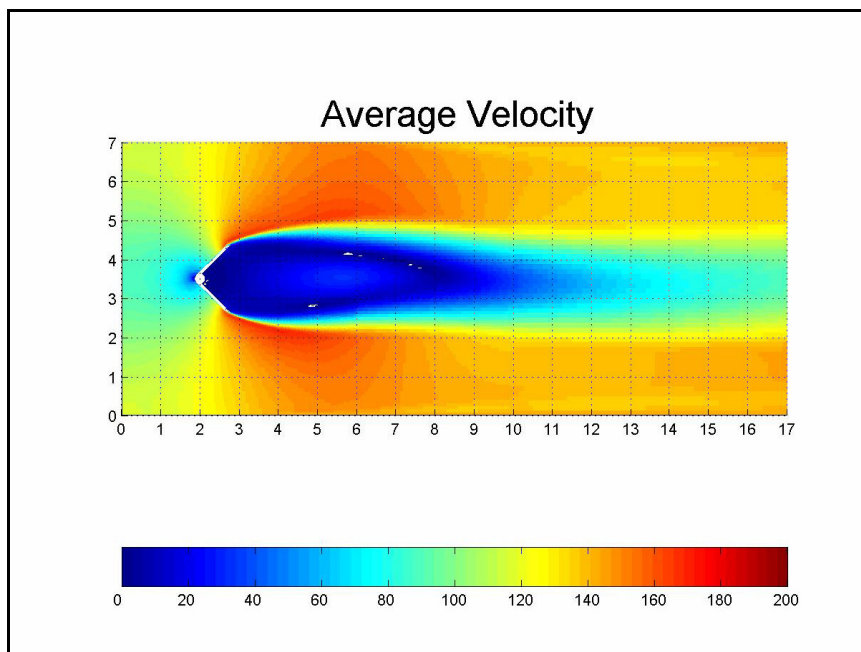


Figure D.3.4 Average velocity values for 90° wedge after 10,000 iterations.

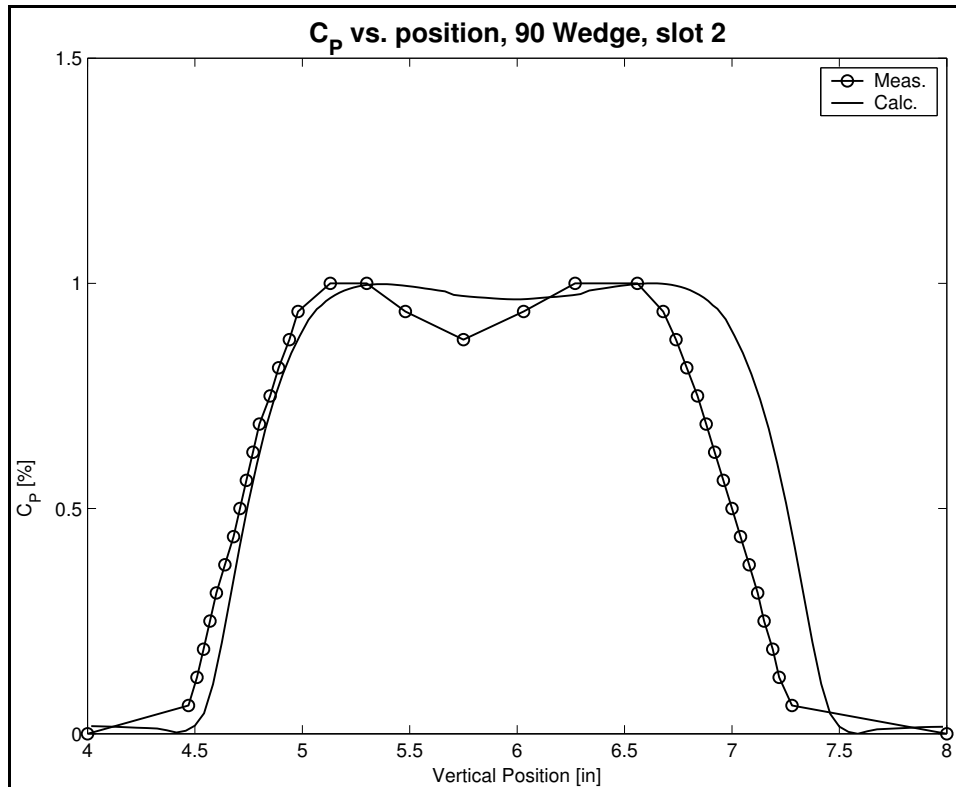


Figure D.3.5 Comparison of pressure coefficient data for 90° wedge. Values were measured at slot two (three inches downwind of the wedge) in the Eddy study and computed by *wind*. The calculated values are the average of three thousand iterations, normalized to the largest measured value of C_p due to the lack of measured maximum pressure data.

D.4 Solution and Convergence, 120° Wedge

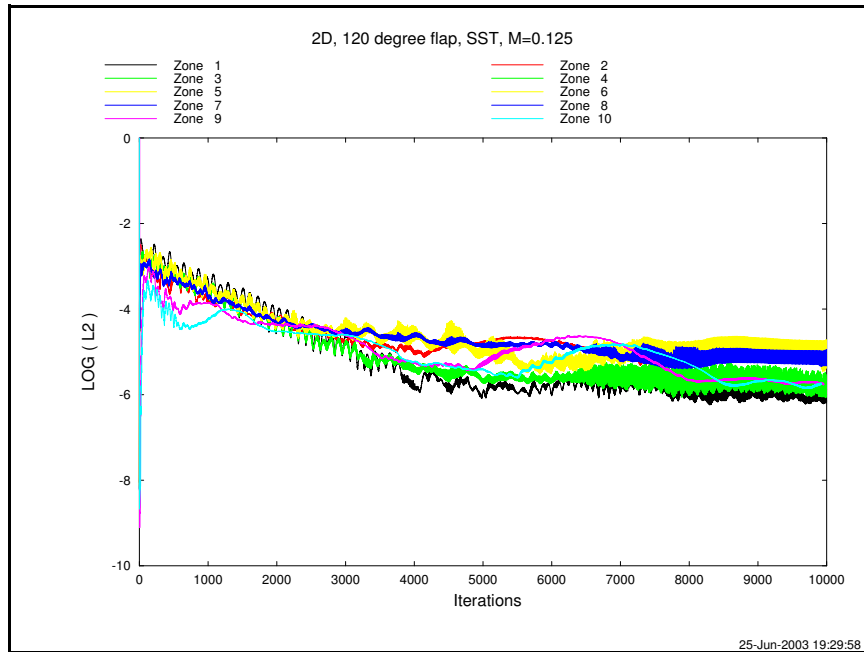


Figure D.4.1 Convergence data for *Navier-Stokes* calculations for the 120° wedge run.

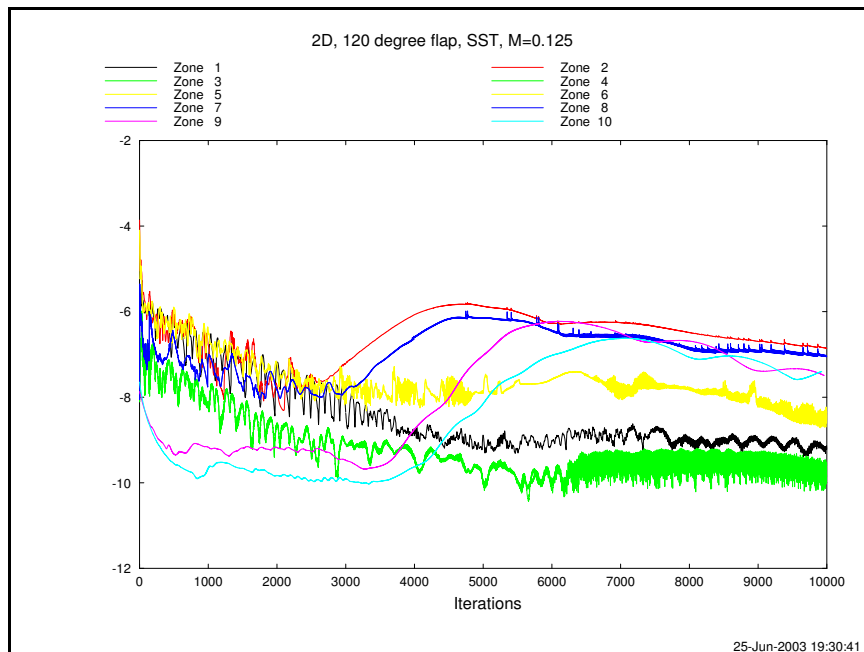


Figure D.4.2 Convergence data for *Shear Stress Transport* calculations, 120° wedge run.

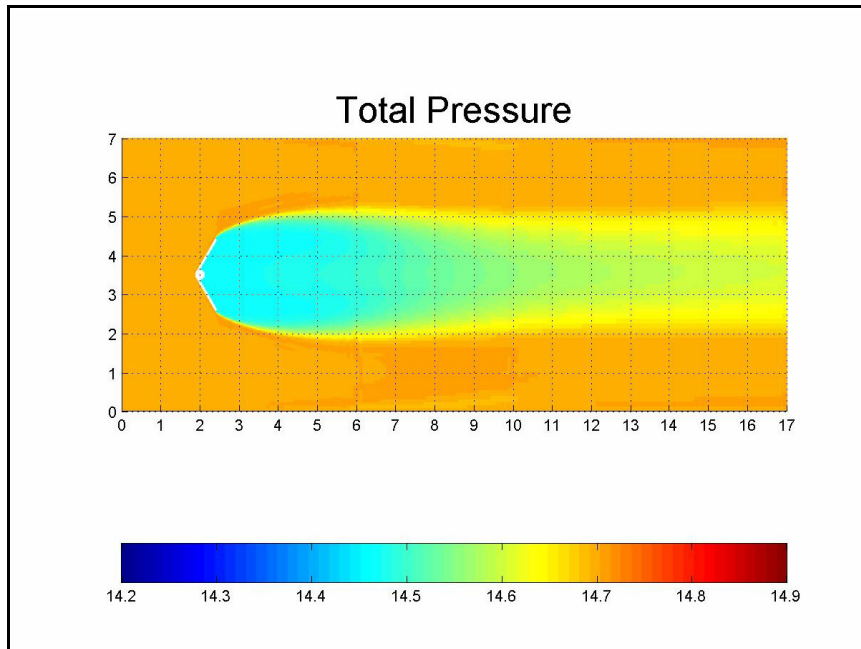


Figure D.4.3 Total pressure values for 120° wedge after 10,000 iterations.

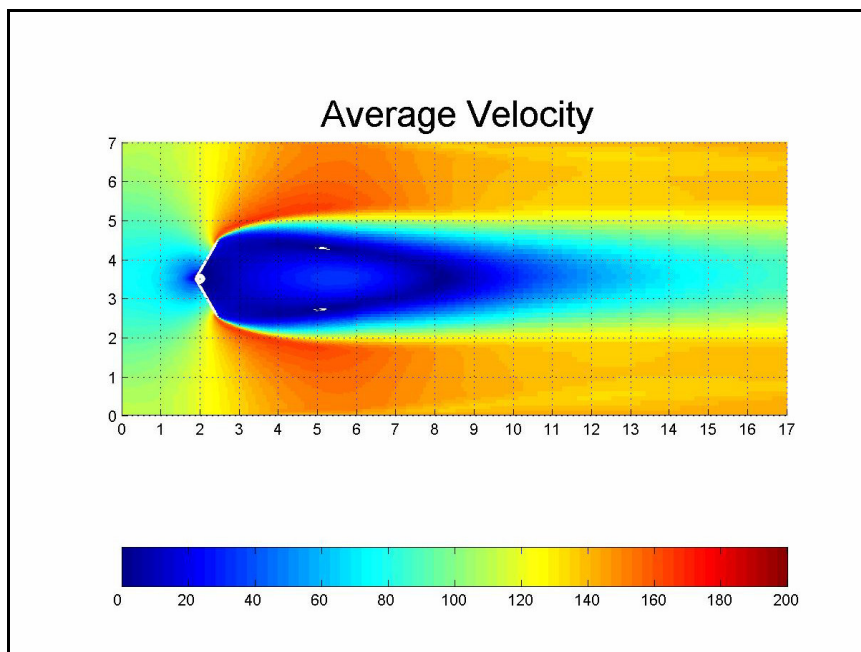


Figure D.4.4 Average velocity values for 120° wedge after 10,000 iterations.

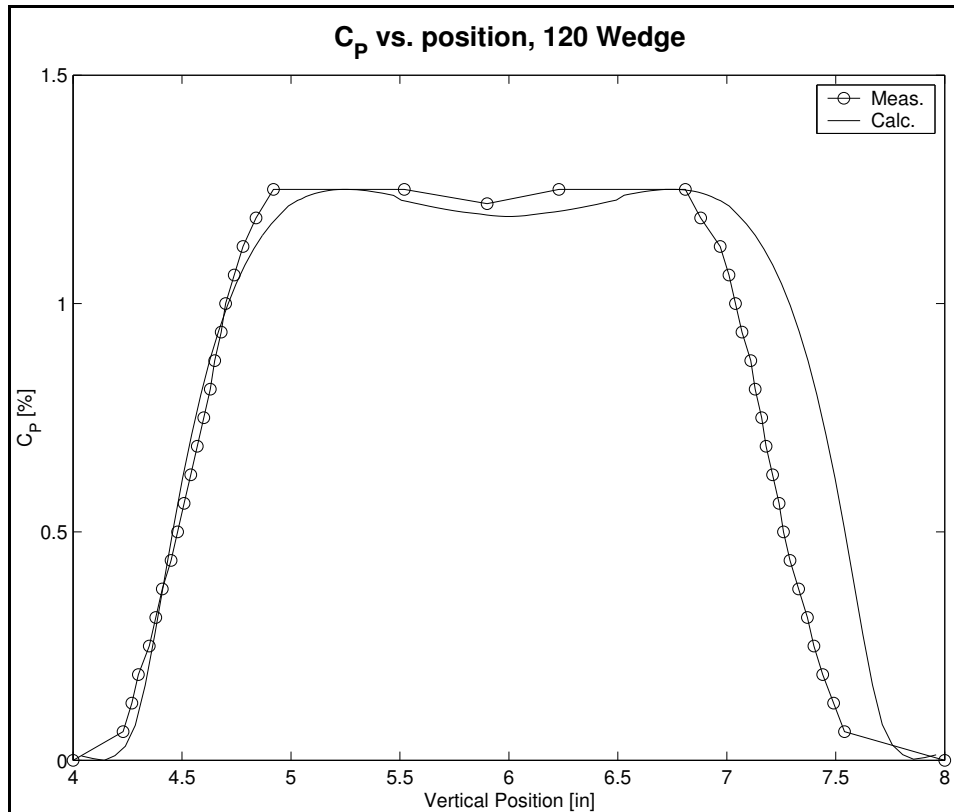


Figure D.4.5 Comparison of pressure coefficient data for 120° wedge. Values were measured at slot two (three inches downwind of the wedge) in the Eddy study and computed by *wind*. The calculated values are the average of three thousand iterations, normalized to the largest measured value of C_p due to the lack of measured maximum pressure data.

D.5 Solution and Convergence, 150° Wedge

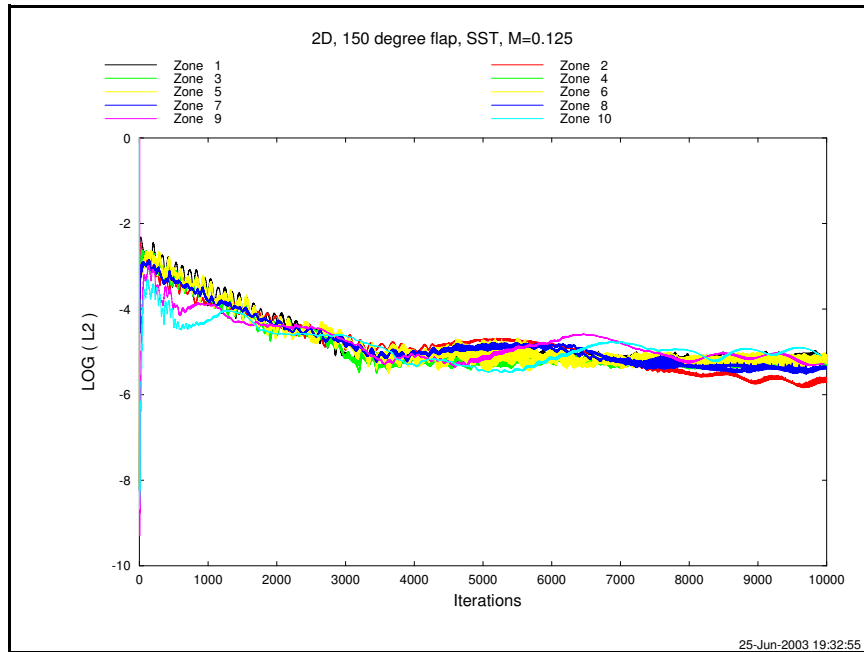


Figure D.5.1 Convergence data for *Navier-Stokes* calculations for the 150° wedge run.

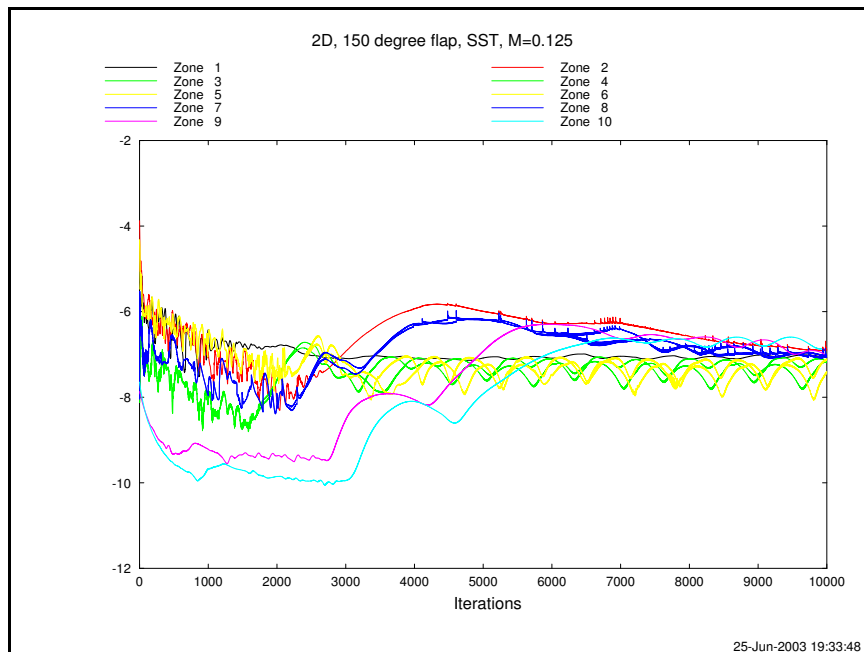


Figure D.5.2 Convergence data for *Shear Stress Transport* calculations, 150° wedge run.

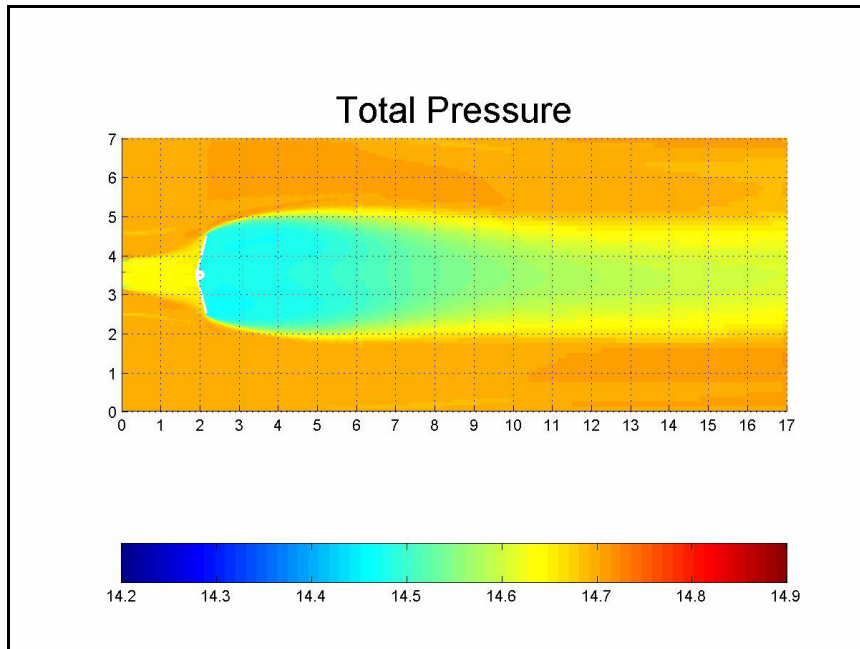


Figure D.5.3 Total pressure values for 150° wedge after 10,000 iterations.

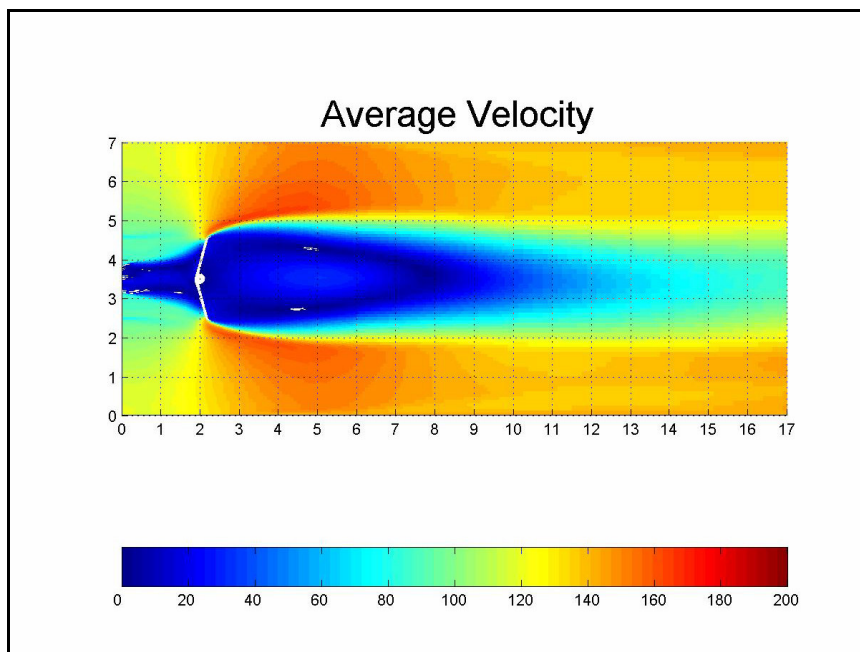


Figure D.5.4 Average velocity values for 150° wedge after 10,000 iterations.

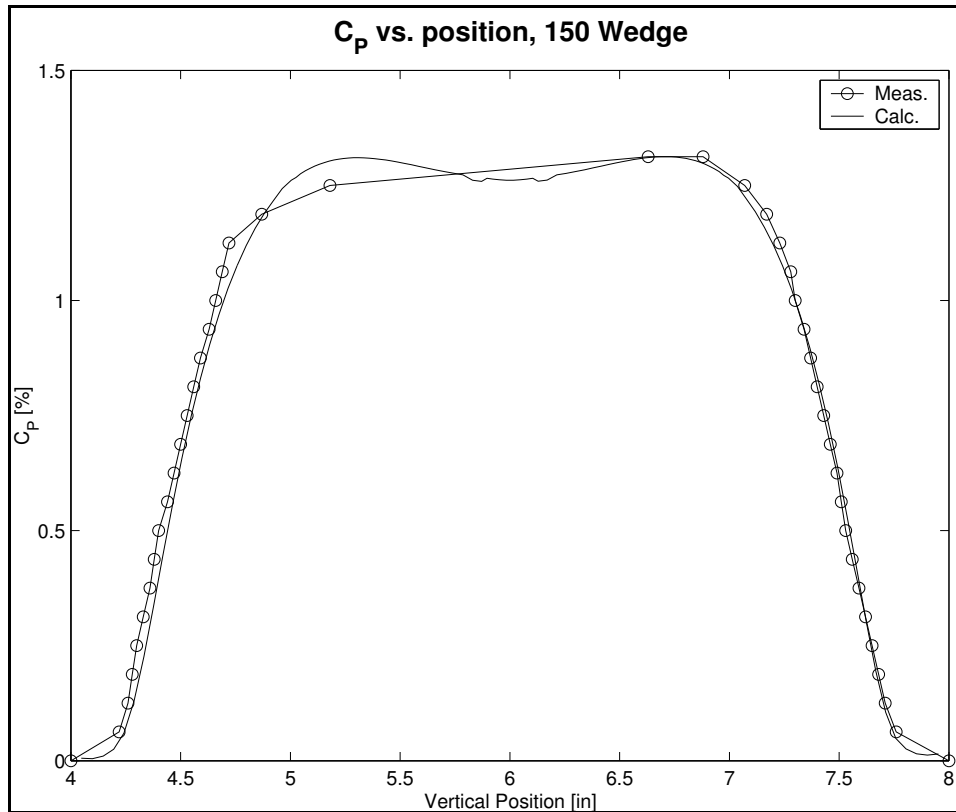


Figure D.5.5 Comparison of pressure coefficient data for 150° wedge. Values were measured at slot two (three inches downwind of the wedge) in the Eddy study and computed by *wind*. The calculated values are the average of three thousand iterations, normalized to the largest measured value of C_p due to the lack of measured maximum pressure data.

Vita

Keith P Savage was born in Williams Air Force Base, Arizona, in 1961. Raised on Air Force bases, he settled down in Colorado after graduating high school. After spending sixteen years working on mainframe computers, he went back to school, receiving his B.S. in Metallurgical and Materials Engineering from Colorado School of Mines in 2001. He is currently pursuing an M.S. in Aerospace Engineering at the University of Tennessee Space Institute.